Faculty of Science and Technology

MASTER'S THESIS

Study program/ Specialization: Risk management	Fall semester, 2015 Open access
Writer: Per Fredrik L. Hemmingsson	*(signature)* Writer's signature)

Faculty supervisor: Professor Eirik B. Abrahamsen University of Stavanger External supervisor(s): Dr. Bjarne Christian Hagen Stord/Haugesund University College

Thesis title: Assessing the model error in flame extensions under ceilings formula with FDS.

Credits (ECTS): 30

Key words: Model, model error, uncertainty, flame extension, FDS, simulation, heat release rate	Pages: 60 + enclosure: 29 Stavanger, 14 December 2015 Date/year

I

Preface

This thesis is the final work in a master degree in Risk management at the University of Stavanger and is credited with 30 ETC points.

I first got interested in Heskestad and Hamada's flame extension formula when I participated in a course in advanced fire dynamics on Stord/Haugesund University College in 2014. The fact that fire engineers used an empirical formula based on seven experiments without questioning it surprised me, and I soon found out that this was something I would like to look closer at.

The work with models, FDS, MATLAB and data analysis in Excel has been interesting and opened my eyes of how we use models and simulations in our daily lives without knowing all the background information about them. When performing work like this it is important to work systematically and to note specific data down directly. When performing a large amount of simulations and processing data it can be hard to remember what has been done and what a specific simulation was named.

I hope this thesis and the work performed can contribute to the discussion regarding the use of empirical models, and the importance of continued studies on flame extensions under ceilings.

Acknowledgements

I would like to thank my supervisor Professor Eirik B. Abrahamsen at UiS for the help with this report and for all the positive feedback, external supervisor Dr. Bjarne Christian Hagen at Stord/Haugesund University College, for always taking time to answer questions and discuss different topics.

I also would like to thank my colleges at Stord/Haugesund University College, PhD student David R. U. Johansen, Assistant Professor Einar Kolstad, Assistant Professor Harald Spångberg and Assistant Professor Gisle Kleppe for their interest, questions, and advice during the project. A special thank you to PhD student Ingunn Haraldseid for all the invaluable help she has given me.

At the end I would like to thank my wife Fatima, our children Fabian and Filip for the support and understanding throughout the process of writing this master thesis.

Abstract

Heskestad and Hamada developed a formula in 1992 to calculate the flame extension from a flame that impinged on a horizontal ceiling. The developed formula was based on seven experiments with a maximum heat release rate of 764 kW. Since 1992 there has been a development of the furniture used in homes, which in turn has led to a larger potential heat release rate from furniture fires. Today a sofa can have a potential heat release rate of 2500 kW. Since the formula is based on seven experiments and the increase of potential heat release rates in furniture fires, it is of interest to investigate if the formula developed by Heskestad and Hamada is accurate for fires with a heat release rate larger than 764 kW.

In this report, the model error of Heskestad and Hamada's flame extension formula is analyzed against simulations performed in FDS for heat release rates between 23.2 kW and 7000 kW. In total 20 simulated results were analyzed against calculations using Heskestad and Hamada's flame extension formula. The results show a standard percentage model error of ±10.8 % between the simulated results and the calculated results using Heskestad and Hamada's flame extension formula. The result including the uncertainties and limitations of the simulations show that the formula for flame extensions under ceilings developed by Heskestad and Hamada, can be used for fires an heat release rate between 23.3 kW to 7000 kW.

Table of contents

Table of figures

X

List of Tables

Definitions

FDS	Fire Dynamic Simulator
CFD	Computational Fluid Dynamics
LES	Large Eddy Simulation
NIST	National Institute of Standards and Technology
DNS	Direct Numerical Simulation
MPI	Message Passing Interface
HRR	Heat release rate [kW]
HRRPUA	Heat release rate per unit area [kW/m^2]
HRRPUV	Heat release rate per unit volume [kW/m^3]
A_f	Horizontal burning area of fuel [m^2]
c_p	Specific heat at constant pressure [kJ/(kg K)]
D	Fuel source diameter[m]
D^*	Characteristic fire diameter
g	Acceleration due to gravity [m/s^2]
$\Delta_G(X)$	Model error
$\Delta_{G_\%}(X)$	Percentage model error
$\overline{\Delta_{G_\%}(X)}$	Average percentage model error
H	Ceiling height [m]
ΔH_c	Complete heat of combustion [kJ/kg]
L	Flame height [m]
L_f	Mean flame height [m]
$\dot{m}''$	Mass burning rate per unit area [kg/(s m^2)]
r_f	Flame radius under ceiling [m]
$s_{\Delta_{G_\%}(X)}$	Standard percentage model error
T_∞	Ambien air temperature [°C or K]
$\dot{Q}$	Energy release rate [kW]
$\dot{Q}^*$	Dimensionless energy release rate
ρ_∞	Ambient air density [kg/m^3]
χ	Combustion efficiency

1   Introduction

1.1   Background

The furniture used in homes has changed over the years. In the 1980's it was not unusual for a sofa in the living room to be made out of skin or leather. These materials are difficult to ignite, and it is not unusual to see an old leather chair with burn marks from cigarettes. Today the furniture's are larger and are made and filled with synthetic materials. In England upholstered furniture is treated with a fire retardant to minimize the fire hazard. This however is not allowed in Norway, since some of the chemicals used are cancerous. With larger more synthetic furniture in Norwegian homes the potential fire effect has increased. An ordinary corner sofa can have a potential heat release rate from a fire of 400 kW/m^2 floor area it occupies. A large sofa of 6 m^2 can then have a total potential heat release rate of 2400 kW, which is equivalent of the heat release rate of a small car.

The production both oil and gas on offshore and onshore installations are also increasing. There are larger amount of gas transported in pipelines under higher pressures. Many of these pipelines go through enclosed modules, and an ignited leak from such a pipeline could lead to a very large fire, that could affect the surrounding modules.

Both these scenarios are fires that can occur under a ceiling. When a flame impinges on a ceiling it can result in a flame extension. Flame extensions under ceilings are not widely studied. In 1981 a report was presented by You and Faeth (1) where they investigated how a fire that impinged on an horizontal ceiling behaved. There experiments were small scale and with small fires and low ceiling heights. In 1992 Heskestad and Hamada (2) continued this research with larger fires up to a heat release rate of 764 kW and higher ceiling heights than You and Faeth. Heskestad and Hamada's seven performed experiments lead to an empirical formula (1.4) that is used today (3) for calculating flame extensions under ceilings.

The small amount of experiments performed by Heskestad and Hamada when developing their flame extension formula (1.4), and the low heat release rate by today's standards, allows the validity of the formula to be questioned for the use of fires with an heat release rate higher than 764 kW. It is therefore of interest to assess the model error of Heskestad and Hamada's flame extension formula for fires with a heat release rate larger than 764 kW.

1.2   Purpose and research questions

The purpose of this master thesis is to assert the model error of Heskestad and Hamada's formula (1.4) for flame extensions under ceiling with the use of FDS, for fires with a heat release rate between 23.2 kW and 7000 kW.

In this thesis the following questions will be investigated:

1. Can simulations perform in Fire Dynamic Simulator (FDS) be used to calculate flame extensions under ceilings?
2. Can Heskestad and Hamada's flame extension formula (1.4) be used on fires with a heat release rate between 23.2 kW and 7000 kW, based on the model error against simulations performed in FDS?

1.3 Structure

This thesis is divided in to seven chapters. Chapter 1 will give an introduction and background to the thesis. It will also give the purpose of the thesis and the research questions related to the research in this thesis.

Chapter 2 describes the most relevant theories for the areas of fires and models. There will also be given a short introduction to the programs used in the simulations and data analysis.

How the simulations were setup in FDS will be explained in chapter 3, together with the MATLAB script used to calculate the results.

The results from the simulations in FDS will be presented in chapter 4. The chapter will also present the results from the comparison between the simulation results and hand calculations using the equation presented by Heskestad and Hamada.

In chapter 5 the results from the simulations and calculations will be discussed.

Chapter 6 will give a conclusion of the discussion in chapter 5, and further work will be presented in chapter 7.

2 Theory

This chapter will give a short introduction to the most relevant theories regarding fires and models. The theories are meant to give the reader an understanding of what this thesis is founded on, and some important facts regarding the work performed.

2.1 Fire theory

2.1.1 Enclosure fires

A fire in an enclosed space can develop in many ways. How an enclosed fire develops is dependent on several factors (3):

- Geometry of the enclosure
- Ventilation
- Fuel type
- Amount of fuel
- Surface area of the fire

An enclosed fire in its initial stage is fuel controlled and the enclosure does not affect the fire development (3). During the growth of the fire it will release energy. The amount of energy the fire releases can be calculated using equation (1.1) . The fire also releases particles, toxic and nontoxic gasses to the surrounding area, the release of gasses and solids will from here on be referred to as smoke. The flames and the smoke it releases is called the fire plume, this will be more described in chapter 2.1.2 and 2.1.3.

$$\dot{Q} = A_f \dot{m}'' \chi \Delta H_c \qquad (1.1)$$

The fire will produce smoke that will rise to the ceiling due to the density difference between the smoke and surrounding air. The smoke will create a layer of smoke beneath the ceiling called a smoke layer. The behavior of the smoke layer is dependent on the amount of fuel the fire has and the ventilation of the enclosure. If the space that the fire is developing has no ventilation, the smoke layer will propagate down as shown in Figure 1. This will starve the fire of oxygen and the fire will die out (3). If the enclosure however has any kind of ventilation, the fire will continue its development. During this development the fire plume will increase its size, as long as it has access to fuel and oxygen. After a while the fire plume will have grown so large in size it will hit the ceiling, and flame extensions to the sides of the plume will occur (3). This occurrence is described in chapter 2.1.4.
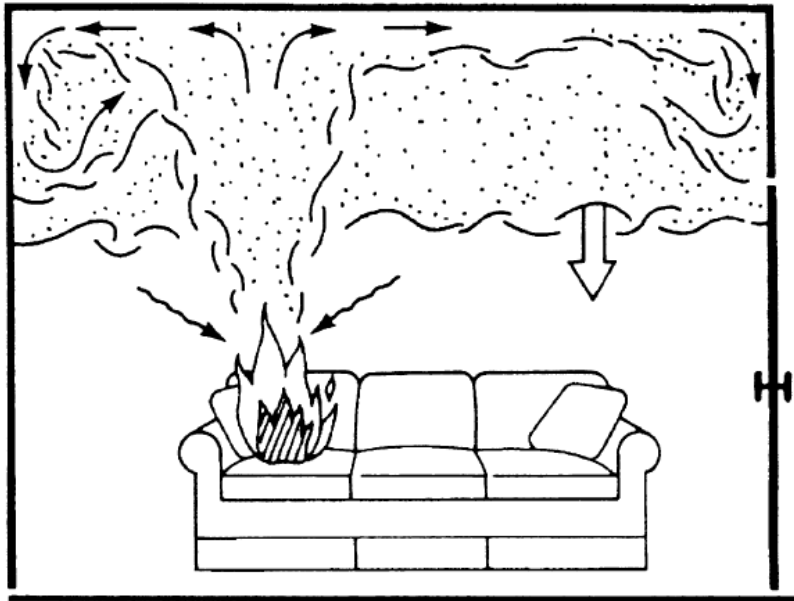
Figure 1 Schematic of descending smoke layer (3)

If the fire is left undisturbed the temperature in the enclosed compartment will reach 500 - 600°C, and there will occur a flashover. Flashover is the rapid transition from the growth phase of a fire, to a fully developed fire, this transition is illustrated in Figure 2 (3). When a fire reaches this phase it is at its largest. It will from here go a fuel controlled fire, to a ventilation controlled fire with temperatures in the enclosed room ranging from 700 to 1200°C. It is not unusual to see flames coming out of the opening of the room when it is in this phase (3).

Figure 2 Description of temperature variation with time in an enclosed fire (3)

After a while the fuel the fire is dependent on will start to diminish. With this the energy the fire develops will lessen and the temperature in the room will start to decrease. The fire now enters the decay phase and can here go from ventilation controlled to a fuel controlled fire. When the fuel for the fire is consumed the combustion producing flames will end (3).

4

2.1.2 Diffusion flames

There exist two types of flames: premixed- and diffusion flame. The main difference between these two flames is how fuel and air is mixed. In a premixed flame the fuel and air is mixed before the mixture is combusted, and in a diffusion flame the mix of fuel and air occurs in the zone of combustion (4).

Diffusion flames are a common flame in the world of safety engineering. Diffusion flames comes from when a volatile such as gas, liquid or solid materials are exposed to enough energy in the form of heat to release combustible gases, which can be ignited together with air. Due to the convection from the heat to the gasses, the gasses will rise upward leading to a buoyant flame. Since fuel and air is mixed in the combustion zone of the flame, turbulence is formed as eddies in and around the flame. The turbulence leads to a fluctuation in the diffusion flame that can be observed. The turbulence induced fluctuation is the cause to the flames that can be observed "leaping" of the flame as shown in Figure 3. The mixture of fuel and air with its resulting turbulence and buoyance is the cause to the non-homogeneous flame that a diffusion flame is (5).

Figure 3 Picture of diffusion flame from experiments performed by Mats Flo on HSH

2.1.3 Fire plumes and flame height

When hot gasses including flames rise upward due to buoyancy, it is referred to in the literature as a fire plume (3). This is widely studied and there are many theories developed regarding fire plumes. Many of these theories are developed from the ideal fire plume as the reference for their development. There are several of the theories that take their basis from the ideal fire plume and are further developed with the use of experiments, as for example by, Zukoski, McCaffrey and Heskestad. The plume theory developed by Gunnar Heskestad is today one of the most used and can be used for most fire sizes (3).

From the plume theory Heskestad developed a formula to calculate the mean flame height of a fire. Since the fire plume is buoyant and turbulent the flame height will fluctuate over time as shown in Figure 4. The height of the flame is dependent on what size the fire has, and how much total energy it releases (3).
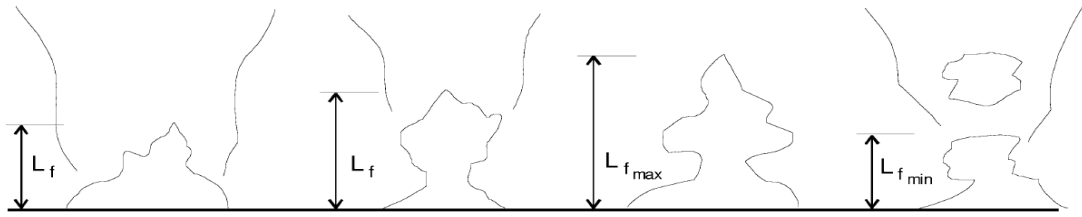
Figure 4 Flame height fluctuation (3)

This formula called Heskestad flame correlation formula is presented in equation (1.2).

$$L_f = 0.235 \dot{Q}^{\frac{2}{5}} - 1.02 D \tag{1.2}$$

Here L_f is the mean flame height [m], $\dot{Q}$ the total energy release rate [kW] and D the diameter of the fire [m].

2.1.4   Flame extensions under ceiling

In some instances the flame of an enclosed fire will be so large that they hit the ceiling of a room. When this occurs it is called that the flame impinges on the ceiling. When the flame impinges on an unconfined ceiling, hot gasses from the flame will spread out under the ceiling as shown in Figure 5, and the gasses from the fire will then spread out radially, and entrain air for combustion, and a circular flame will be formed under the ceiling as shown in Figure 6. The extension of this circular flame under the ceiling is of interest when calculations of the radiative heat transfer from the fire to objects in the enclosed spaced is being performed. (3).
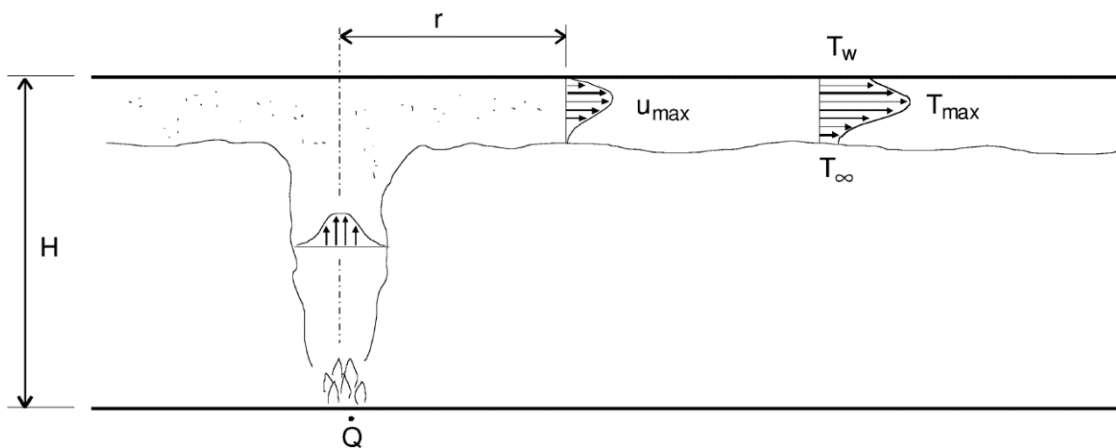
Figure 5 Illustration over flame impingement on ceiling (3)

Flame extension under ceiling is not widely studied. You and Faeth presented a paper in 1981 (1), were they had performed experiments on the radial flame extension under a ceiling. These experiments were performed on small flames with low energy release rates and low roof heights. You and Faeth flame extension equation is given in equation (1.3) (1).

$$\frac{r_f}{D} = 0.5 \left(\frac{L - H}{D} \right)^{0.96} \tag{1.3}$$

Equation (1.3) is intended for rough estimates of the flame extension under ceiling, due to the use of small scale fires and low ceiling heights in the experimental setup.

In 1992 Heskestad and Hamada presented an equation (1.4) based on 7 experiments with a larger heat release rate and greater roof heights than the experiments performed by You and Faeth (2).

$$r_f = 0.95(L - H) \qquad (1.4)$$

The heat release rates in the experiments ranged from 23.3 kW to 764 kW, and the roof height from 0.56 m to 1.51 m. Two experiments with different roof heights were performed with 764 kW heat release rate. One with a roof height of 0.92 m and one with 1.51 m roof height (2).
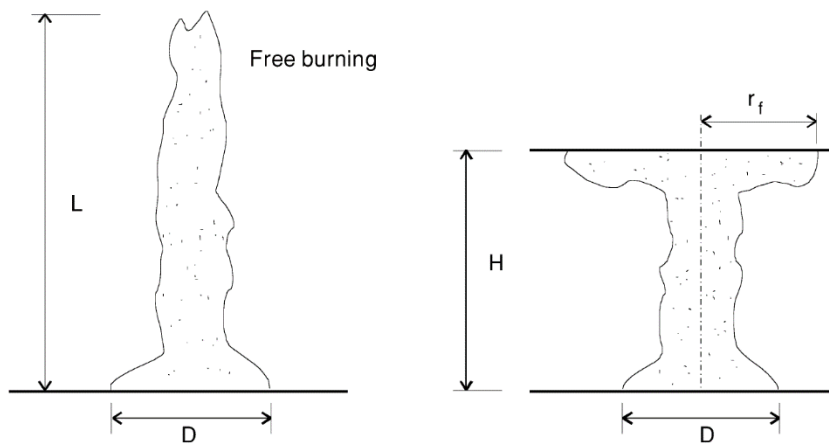
Figure 6 Flame extension under ceiling

Heskestad and Hamada do not present any experimental results for the length of the flame extension radius in their paper. The only results that are presented is the constant 0.95, that is derived from the mean flame ratio L_r, to the free flame portion intercepted by the ceiling $L_{fr} - H$. The ratio ranged from 0.88 to 1.05 in the experiments, giving an average of 0.95 (2).

In the literature it is stated that equation (1.4) may provide a more realistic estimate for the flame extension radius for larger flames than equation(1.3). It is also stated that more experimental data is needed as evidence to support equation (1.4) (3).

There have been done other studies than these two on the flame extension under ceiling radius. Among these are an integral model developed by Ding and Quintiere (6). This model is developed from the equations presented by You and Faeth, Heskestad and Hamada and a Ph.D dissertation by Y. Yokobayashi in Japan. This is an interesting model, however since it is not based on new available experimental results, it is not included in this report (6).

As presented in the beginning of this chapter, if a flame impinges on an unconfined ceiling a radial flame will be produced. This implies that the geometry of the roof is of importance. If the fire would be in a corner or up against a wall, the radial flame would be confided by the walls as shown in Figure 7. The flame extension from such a fire could not be calculated using Equations (1.3) and (1.4).
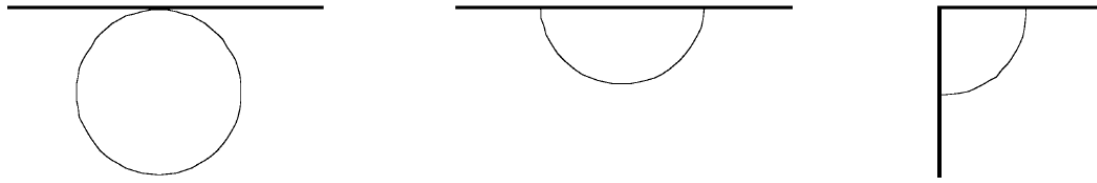
Figure 7 Fire sources near a wall or in a corner

One other circumstance that can occur is that of a fire in a tunnel. In a tunnel the roof is often curved and there is forced ventilation pushing the air in the tunnel in a certain direction. The forced ventilation would not only push the air in a certain direction, but also the flame extension as shown in Figure 8, producing a flame extension that would be longer in one direction and not radial divided in all directions (7).
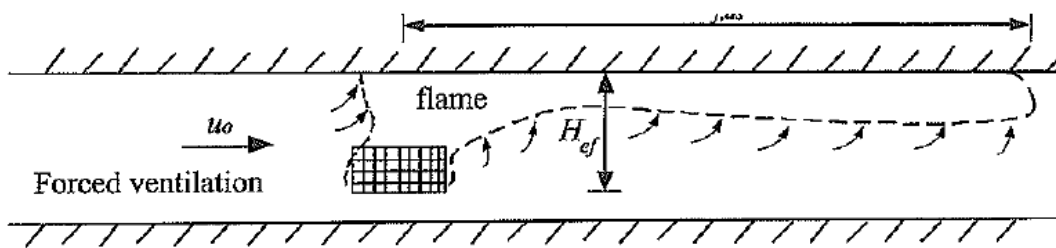
Figure 8 Flame extension under ceiling with forced ventilation (7)

2.2   Models

Mathematical models are commonly used when performing risk analysis or working in the field of fire safety engineering. It is important to understand what a model is and what results its use will give.

Oxford English Dictionary defines the word model depending on its indented use. It defines a mathematical model as (8):

> "*A simplified or idealized description or conception of a particular system, situation, or process, often in mathematical terms, that is put forward as a basis for theoretical or empirical understanding, or for calculations, predictions, etc.; a conceptual or mental representation of something*"

In risk analysis and fire safety engineering, models are used to for example analyze a system or to simulate how a real event may occur etc. A model is therefore a representation for a simplified version of a system or event. What models that are going to be used to perform the analysis, depends on what results are needed by the user for future work (9).

2.2.1   Models in risk analysis

A system can be said to consist of different subsystems, representing the different parts and levels of the system. An analysis of the system can then be made by analyzing the different subsystems to find how the system will be affected when unwanted situations arise in the subsystems. Like systems, models can be said to consist of different sub models, and these sub models can in turn be analyzed to find problems in the model as a whole. In risk analysis models are in common use, and can be divided in to two categories: quantity-oriented (physical) or event-oriented (logical) models (9).

8

Quantity-oriented models are used to find the value of a quantity *Z* that can be observed in the future. *Z* can be modeled by using the function *G* together with input quantities (parameters) *X* (10). How function *G* is setup depends on the model in use. The function is often based models used in physics, chemistry or models derived from performed experiments (9).

Event-oriented models are logical models that are composed of conditions and logical terms. Event-oriented models outline the conditions for which an event occurs, while quantity-oriented models look at numerical values of different quantities and the result of these. The outcome of event-oriented models is usually binary and can be seen as failure/not failure (9).

2.2.2   Model uncertainty

As presented in chapter 2.2 a model is a representation for a simplified version of the system or event on which the model is being used. Because of this simplification there will be uncertainties connected to the model. The uncertainties connected to the model will be related to the output values the model produces, and the true values X_{true} of the input quantities used in the model. In quantity-oriented models presented in chapter 2.2.2, a quantity *Z* that could be observed in the future could be modeled using the function *G* and the input parameters *X*, giving a model described as *G(X)*. The difference of the model output (prediction) of *G(X)* and the true future value of the observed quantity *Z* will give the model error $\Delta_G(X)$, and can be calculated using equation (1.5) (10)

$$\Delta_G(X) = G(X) - Z \tag{1.5}$$

The model output uncertainty is not the same as the model error $\Delta_G(X)$, but the epistemic uncertainty of the value of the model error $\Delta_G(X)$, and can be assessed by using for example subjective or imprecise probabilities as measures (10).

The combination of two components in the model results in the model output uncertainty: structural model uncertainty and parameter (input quantity) uncertainty (10).

Structural model uncertainty is the uncertainty that occurs when we are certain of the input quantities *X* and know their true value X_{true}. Uncertainties related to the input quantities can then be ignored and the uncertainties are only a factor of the structure of the model *G* (10).

Sources of structural uncertainty can come from little understanding or poor knowledge about the system the model devised for. It can also be a result from a lack of understanding how natural phenomenon's occur, and contributions of other circumstances that has not been taken into consideration. These sources will lead to a "flawed" model structure when the model is devised and give the model a structural uncertainty. Models based on mathematical theories can have structural uncertainties connected to them due to simplifications and assumptions made when the theories are converted to models. Many of the computerized models used today are converted from mathematical theories, and can in turn have uncertainties in the form of errors done in the computer code when the model is converted, and other uncertainties due to computer limitations (10).

Input Quantity (parameter) uncertainty is the uncertainty (due to lack of knowledge) about the true value X_{true} of the input quantities *X*. This means that the uncertainties about the structure *G* can be ignored and the uncertainty are only related to the input quantities *X* and their true value X_{true} (10).

2.2.3 Model sensitivity

Model sensitivity analysis is an analysis on how much the model output are affected from changes in the model input values. This is an examination of the imprecisions or uncertainties in the input values for the model in a decision-making or modeling process. What character of sensitivity analysis that is being performed is dependent on the context and what questions it should answer. This kind of analysis can give an indication of the precision of the model used, and it can also give detailed information about the significance of error in the model input values used. The results from this kind of analysis can be used to identify where efforts should be put to improve the model and its input variables (11).

Methods used in sensitivity analysis are many, divers and can be categorized in different ways. There are mathematical, statistical and graphical models. These models focus on the methodology of a specific technique, while other models rather focus on the capability. In this thesis a mathematical method is used for the sensitivity analysis (12).

Mathematical methods in sensitivity analyses use a variation of the input values to evaluate the sensitivity of the model output. This is usually done by performing calculations of the model output for a few values for one input that span the range of that input. Variance in the output due to variance in the input is not addressed with mathematical methods. However it can assess the impact of range of variation the input values has on the output. Mathematical methods can be used to determine the most significant input quantities in the model, identifying input quantities that can require further work. When performing validation or verification of a model, mathematical methods can be used (12).

2.2.4 Validation

Validation is a derivate of the verb validate which means to "*demonstrate or support the truth or value of*" according to Oxford Dictionary of English (8). There are various definitions today of what a model validation is, and since there are different models, there are several different ways to validate them (13). Most however define model validation as the process were the mathematical model the model is built on is checked to be appropriate for the physical model it is meant to represent. This determines how well the model predicts the actual physical phenomena of interest (14).

The validation process is usually preformed in several steps (14):

1. Compare the results from the model with experimental results.
2. Quantify the differences of the model results and experimental results in light of their uncertainties.
3. Determine if the model is suitable for its intended use.

Since validation is seen as a process, it does not have a final endpoint. The validation process is continued as long as new information or knowledge comes in to existence in the intended area for the model (13).

This validation process presented above is very common for CFD programs. CFD programs are used in fire safety engineering to help protect individuals, infrastructure and the environment by predicting the behavior of fires and to simulate fire scenarios. This makes the validation process important for fire safety engineers regarding the output results of the CFD programs. By reading the documentation of the validation process for the CFD program, and checking if the process performed

is good enough for the intended use of the model, the "goodness" of the output results can be decided. This is always the end user of the programs responsibility (14).

CFD programs are also used in research work today. The programs can then be used to predict outcomes of physical events that have no experimental data. This can be because the programs are used to model situations that has not yet occurred, or there could be difficulties to replicate the scenarios the models predict in reality. The user would then need to look at the validation process performed on the program for similar situations and make a judgement if the process and its results are good enough to be used in that situation (13).

2.3   Fire dynamic Simulator

FDS is a CFD model, used for calculating fire-driven fluid flow using the Navier-Stokes equations. These equations are appropriate for the low-speed flow that occurs in a buoyance driven flow from a fire with the emphasis on the smoke and heat transport the fire produces (15).

The model is today used for designing smoke handling systems, sprinkler/detector studies and residential and industrial fire reconstruction. Since FDS first was released in February 2000 the goal for the development of the model has been to create a model that can solve fire problems in the area of fire protection engineering, and to provide a tool for the study of fundamental fire dynamics and combustion (15).

Some of the important features in are:

Hydro dynamic model FDS solves the fire-driven fluid flow with a form of the Naivier-Stokes equation. The core algorithm used for this is an explicit predictor-corrector scheme which is second order accurate in space and time. The turbulence flow in FDS is solved by using Large Eddy Simulation (LES). This lets FDS solve the large eddies created by the turbulence in the simulation, the smaller eddies that cannot be solved with LES is solved with the use of the Navier-Stokes equation. If the mesh of the simulation is fine enough, there is a possibility to use Direct Numerical Simulation (DNS) to solve the calculation of the turbulence, but LES is the default model used by the program (15).

Mesh and Grid When setting up a simulation in FDS the user specifies a mesh or multiple meshes for the simulation. The size of the spacing in the mesh or meshes for the simulation is specified as the grid size in the setup. If the mesh has a uniform grid size Figure 9 only one mesh and grid size needs to be specified in the setup of the simulation. If the simulation on the other hand has multiple meshes as illustrated in Figure 10, each of the mesh needs to be specified separately. When using multiple

Figure 9 Uniform grid size one mesh setup in FDS

meshes there is a possibility in FDS to use different grid sizes on the meshes. In that case is it important that the sizes of the meshes align and have the same cross sectional area (Figure 11) (15).
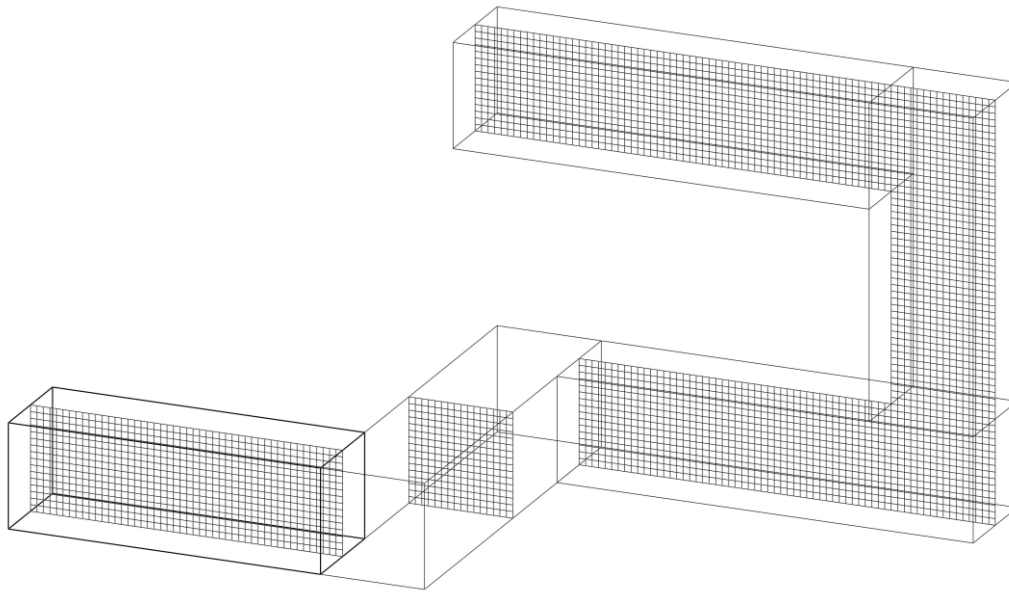
Figure 10 Multiple mesh simulation in FDS
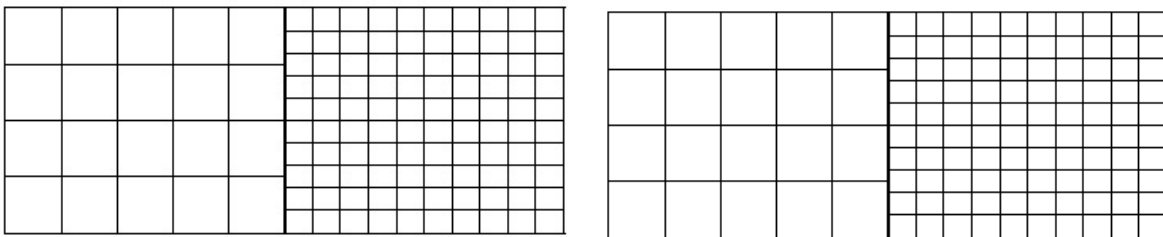
Figure 11 Unaligned and aligned mesh in FDS

Geometry Since simulations in FDS are run with a rectilinear mesh, the geometry of the setup simulations must conform to the underlying mesh. This means that obstructions or other geometry in FDS that has another shape than squared will be adapted to a square geometry by the program (15).

Parallel Processing FDS has the possibility to use multiple processor units on a computer to solve a simulation (15). This is done with the use of OpenMP (16). With the use of OpenMP, FDS divides the simulation in to equal parts as the number of processors the simulation will be run on. The number of processors to be used in OpenMP is chosen by the user and the number of processors used will speed up the simulation to a point. For example, using 8 cores instead of 2 will probably increase the simulation speed with a factor of 2. The other option is to use MPI. This lets the user setup the simulation using multiple meshes and choosing which mesh should be run on which computer. This is normally in use when clusters of computers are available for simulation work (15).

2.3.1 Important parameters in Fire Dynamic Simulator

When setting up a simulation in FDS there are certain parameters that are important to minimize the uncertainty in the output results. Some of these will be presented here and how they are calculated.

Dimensionless energy release rate $\dot{Q}^*$ is a very important parameter in controlling the geometry of fire plumes and in the research on flame height. This parameter will be less than 10 in most fires, and less than 2 in larger fires. Experiments have shown that the normalized mean flame height $\left(L_f\right)$ correlates well with a $\dot{Q}^*$ in the range $1<\dot{Q}^*<1000$. It is therefore of importance that the value of $\dot{Q}^*$ is greater than 1 in simulations performed in FDS with regards to flame height. The parameter $\dot{Q}^*$ can be calculated using equation (1.6) (3).

$$\dot{Q}^* = \frac{\dot{Q}}{\rho_\infty c_p T_\infty \sqrt{gD} \cdot D^2} \tag{1.6}$$

Characteristic fire diameter D^* is the effective fire diameter of the fire, based on the heat release rate. It can be calculated using equation (1.7).

$$D^* = \left(\frac{\dot{Q}}{\rho_\infty c_p T_\infty \sqrt{g}}\right)^{\frac{2}{5}} \tag{1.7}$$

Grid cell size δ_x. This represents the characteristic size of a grid cell in X direction.

2.4 Validation of Heskestad flame height correlation formula in FDS

Heskestad flame correlation formula (1.2)has been validated for FDS. This was done by finding the distance above the burner which 99 % of the fuel has been consumed compared with results from performed experiments. The method of finding the distance were 99 % fuel has been consumed is the same as, the distance above the burner were 99 % of the total heat release rate from the fire can be found. This method is admittedly arbitrary (14) when flame height results from FDS are compared to experimental results. The results from experiments performed on Heskestad flame height correlation formula are often based on measures of the radiation emissions from soot (luminosity) the flame produces. The result from different experiments using luminosity as the measurement to find the flame height varies significantly. This variation is especially noted at low values of $\dot{Q}^*$ were the way the burner is configured is important (14).

The validation team also presents results for the distance above the burner were 95% of the fuel had been consumed. This method was used to find the lower boundary for the simulated results using the 99% fuel consumption method (14).

Simulations in FDS performed by NIST, and experiments performed by Tamanini Factory Mutual with a $\dot{Q}^*$ ranging from 0.1 to 10000 were analyzed in the validation. The simulations in FDS were performed with three different resolutions, 5, 10 and 20 that can be characterize with the use of equation (1.8). The resolution gain from equation (1.8) can be seen as the number of grid cells that span the effective fire diameter. The results from the simulations with three different resolutions were then compared to the experimental results (14). The results from FDS were calculated in MATLAB using a script developed by Randall McDermott (17).

$$\frac{\mathrm{D}^*}{\delta \mathrm{x}} = \text{resolution} \qquad (1.8)$$

The comparison of the results shows that when the numerical grid is refined the predicted spatial distribution of the energy release is improved. Giving the use of this method of finding the distance of were 99% of the fuel has been consumed from simulations performed in FDS, with results from Heskestad's flame correlation formula an uncertainty (maximum variation) of ±15 % for fires with a $\dot{Q}^* > 1$. If however the $\dot{Q}^* = 0{,}1$ the uncertainty is approximately ±65 % (14).

3 Methods

To assess the model error for equation (1.4) for the heat release rates of Heskestad and Hamada's experiments, and outside the experimental range of these experiments, it was determined that a computerized model was the best choice. This since there is no nearby facilities that can handle an enclosed fire of 764 kW or larger under controlled conditions. The choice of FDS as the CFD program was based on that FDS is open-source software available for download. This makes the program available for any user that would try to reproduce the simulations performed. FDS is also a widely used CFD program for performing simulation of this type of fires, and is seen as one of the most advanced CFD programs for this use.

3.1 Limitations regarding simulations and calculations

Before a plan for the simulations of the flame extension under ceiling can be made, limitations and applied solutions to these must be found. The limitations considered are listed below in point 1-7:

1. Deciding what method should be used for determining the length of the flame extension.
    A. A measurement for the position where 99 % of the heat release rate is.
    B. Measuring the area where the flame temperature is higher than 550°C.
2. Decide the simulation time.
3. Decide which model of roof temperature that should be used
    A. Full heat transfer model through the roof.
    B. Constant temperature on the underside of the roof at 20°C.
    C. Constant temperature on the underside of the roof at 600°C.
4. Grid sensitivity analysis
5. Decide the effect for experiments outside 764 kW

Before any simulations could be run, a decision on which method A or B for measuring the flame extension length had to be made. Method A is used in the validation of Heskestad flame correlation formula (14). This gives this method more credibility to use, and there is documentation on how the method was used. How the method was setup and used is presented in chapter 3.2. Using method B gives certain problems. To be able to find the area where the temperature of the flame is 550°C (18), a slice file was going to be placed under the ceiling of the simulation. A slice file give the temperature for a very thin slice of the simulation in x, y and z direction chosen making its placement crucial. Since the thickness of the flame extension is not known, were to place the slice file could be hard to ascertain, and the results from this model could not be trusted. It was determined to use method A since it is used successfully to determine flame height, and since the placement for the slice file in method B introduces a new uncertainty, this method was deemed less suitable.

Three 764 kW simulations were run for 100 seconds, and the results from these simulations are shown in Table 1 and Figure 12. The setup of the simulations performed in FDS is presented in chapter 3.2, and the calculations performed in MATLAB in chapter 3.3. The results of the flame extension with the three roof temperature models showed a small deviation, the method with full heat transfer model was chosen.

Flame extension [m]

Time (s)	Full heat transfer model	20 °C	600 °C
10	0.9767	1.0012	0.9695
20	1.0743	1.0923	1.0688
30	1.1106	1.1124	1.1066
40	1.1361	1.1261	1.1353
50	1.1436	1.1397	1.1489
60	1.1409	1.1494	1.1432
70	1.1429	1.1447	1.1491
80	1.1481	1.1433	1.1433
90	1.146	1.1393	1.1435
100	1.1461	1.1417	1.1422
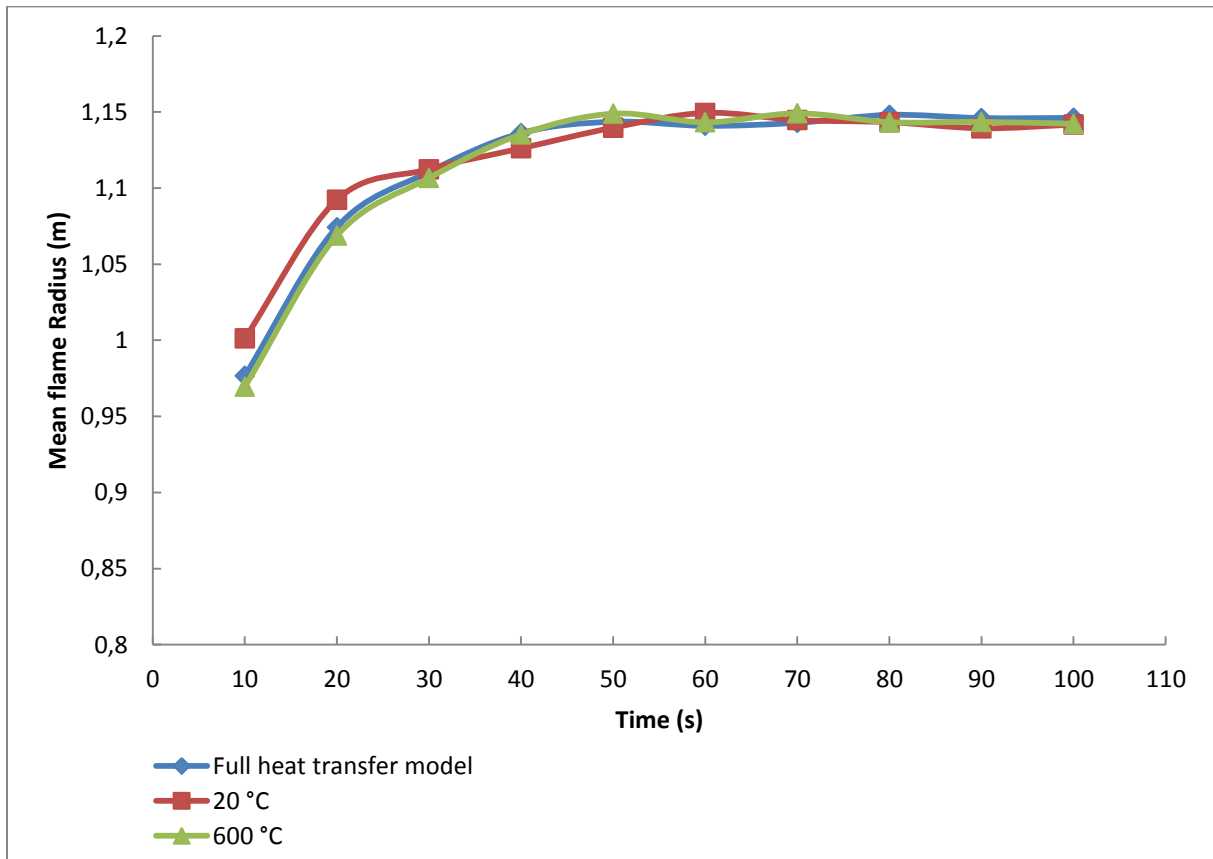
Figure 12 Graph showing mean flame extension for three simulations with different heat transfer models to the ceiling, with an heat release rate of 764 kW and a grid size of 0.0405 m

After the results regarding the choice of heat transfer model had been made, the same results were used to determine the simulation time for the simulations. This decision was made in regard to how long run time each simulation would need on the servers, and how stable the flame extension length was in the simulations. It was concluded from the results from the first simulations that the flame

extension length does not vary in length after 50 s as can be seen in Table 1 and Figure 12. The simulation time were therefore set to simulate over 100 s. The simulations will have a run time on the servers of about 4 – 7 days, this length of time for a simulation was deemed practical.

A grid sensitivity analysis was performed. This was done using simulations with three grid sizes and compare the results with Heaskestad and Hamada's equation (1.4). The grid sizes were set to 0.081 m, 0.0405 m, and 0.02025 m. After four months the simulation with a 0.02025 m grid size was turned off. The simulation had then simulated 47 s of the total 100s simulation time, and it was deemed impractical to continue. The results from the 0,081 m simulation and 0.0405 m simulation are presented in Table 2 and Figure 13. As can be seen from the results, there is a difference of about 34 cm between the two simulations. However the results from the simulation with 0.0405 m grid size correlates with the results given by equation (1.4). It was therefore decided that all simulations on Heskestad and Hamada's equation should be run with this grid size.

Table 2 Results from simulations with a heat release rate of 764 kW and a grid cell size of 0.0405 m, 0.081 m and equation (1.4)

Time (s)	0.081 m grid [m]	0.0405 m grid [m]	Equation (1.4)
10	0.6821	0.9767	1.1515
20	0.756	1.0743	1.1515
30	0.7864	1.1106	1.1515
40	0.7952	1.1361	1.1515
50	0.8007	1.1436	1.1515
60	0.8047	1.1409	1.1515
70	0.8028	1.1429	1.1515
80	0.8063	1.1481	1.1515
90	0.808	1.146	1.1515
100	0.8091	1.1461	1.1515
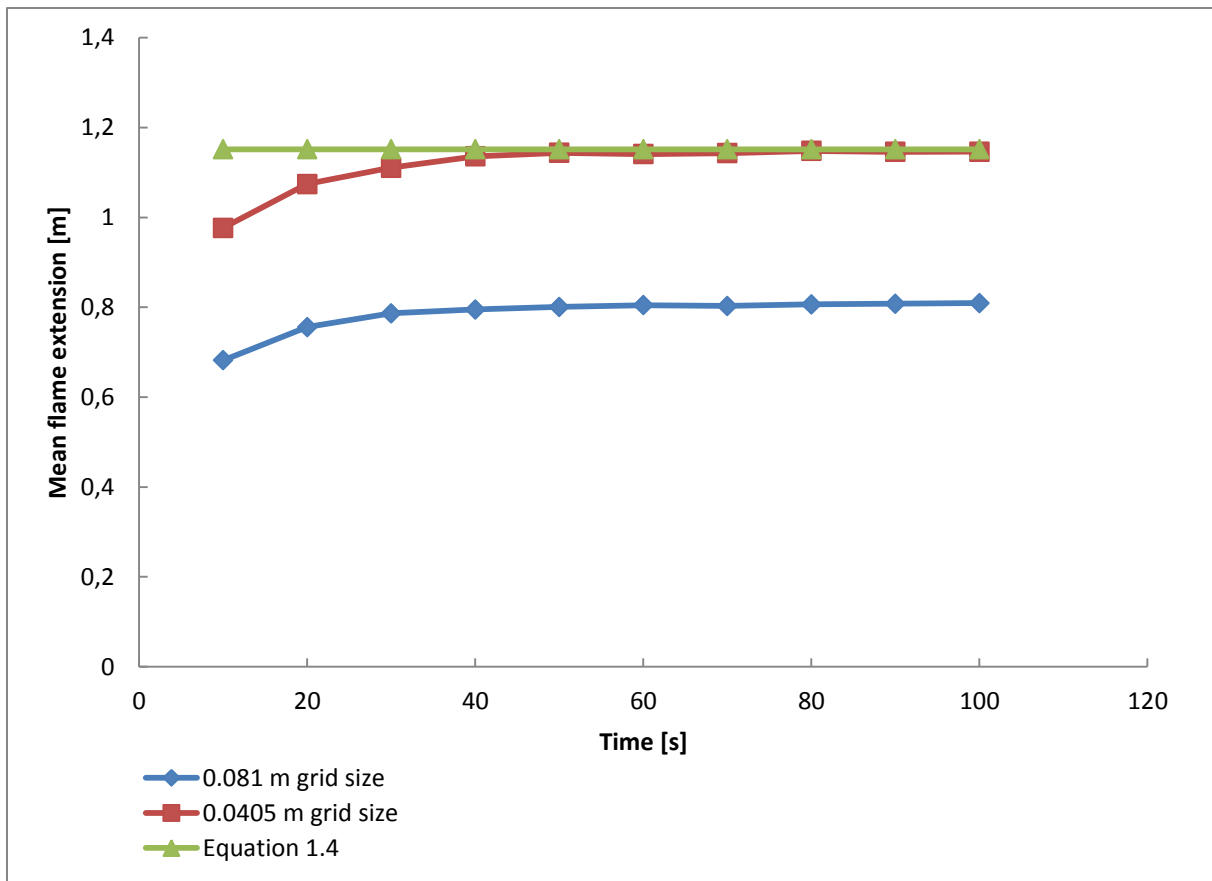
Figure 13 Graph over flame extension length in simulations with a heat release rate of 764 kW and a grid cell size of 0.0405 m, 0.081 m and Heskestad and Hamada's equation (1.4)

The range of the simulation outside the experiments performed by Heskestad and Hamada were decided to be set to 7000 kW with 500 kW increases between each simulation. This would give results for the flame extension length for heat release rates almost 10 times as large as Heskestad and Hamadas experiments. The results for the simulations performed on Heskestad and Hamadas experiments and from 972 kW to 7000kW in presented in chapter 4.

After the simulations from 23.2 – 7000 kW was run, a sensitivity analysis of the model was performed. 5 exactly equal simulations at 764 kW where run and the result of the simulation showing the sensitivity of the simulation. These results are presented in chapter 4.

3.2   Setup of simulations in FDS

The simulations were setup in FDS to mimic as closely as possible the setup of Heskestad and Hamada's experiments (2). The same materials valueswere used in the simulations as in Heskestad and Hamada's experiments (2), the properties of the materials used can be found in Appendix A. Some simplifications were made in the setup of the simulations; the legs of the table and the supports for the roof were removed. These do not impact the way the fire behaves, and were only removed reduce processing time. Heskestad and Hamada used circular sandbox burners and an octagonal ceiling (2). Since FDS conforms to a square grid, square burners and a square ceiling were used in the simulations for this reason, as can be seen in Figure 14. As an example of the programing code used for the simulations in FDS, a 764 kW simulation is presented in Appendix B. In the setup of

the simulation codes a MATLAB script were used for placing the devices measuring the HRRPUV (Heat release rate per unit volume). The script used is presented in Appendix C.
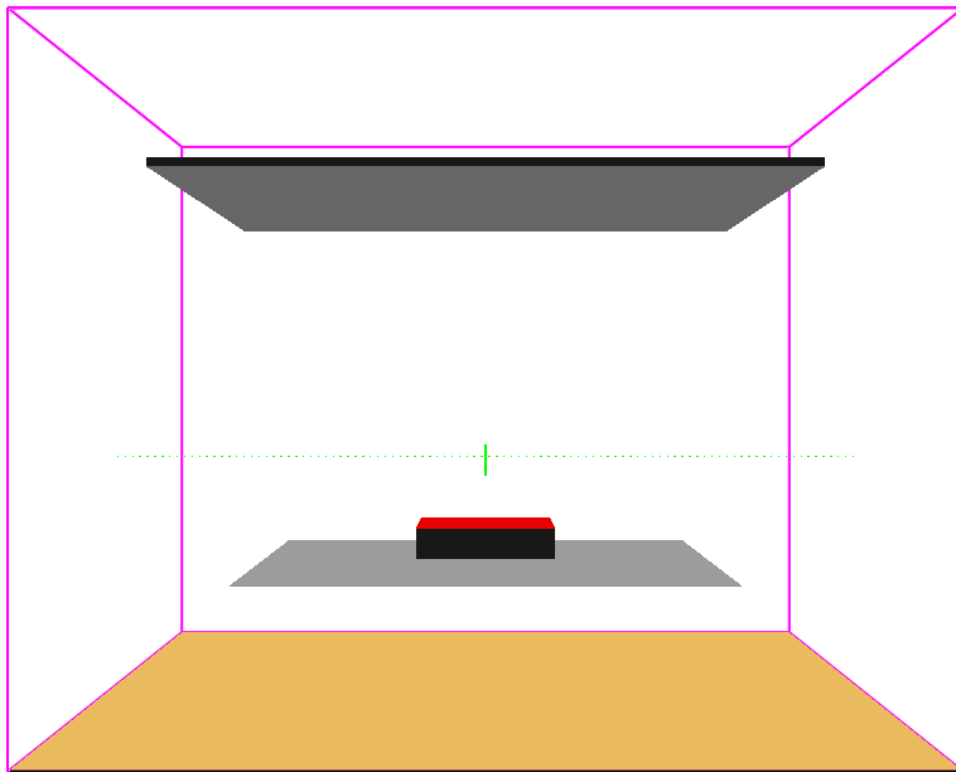
Figure 14 Screenshot of 7 000 kW fire simulated in FDS from Smokeview

In total 60 simulations were run in FDS. The effect, burner diameters, ceiling heights and grid cell sizes of the simulations for mean flame extension length performed in FDS is presented in Table 3. The same effects, burner diameter and grid cell size used in the simulations for mean flame extension length, were used when simulation the mean flame height.

Table 3 Effect, burner diameter, roof height and grid size for performed simulations

Number	Effect [kW]	Burner diameter [m]	Roof height [m]	Grid cell size [m]
1	23.2	0.15	0.56	0.0405
2	46.2	0.15	0.56	0.0405
3	92.6	0.30	0.92	0.0405
4	185	0.30	0.92	0.0405
5	382	0.61	1.51	0.0405
6	764	0.61	1.51	0.0405
7	764	0.61	0.92	0.0405
8	764	0.61	1.51	0.081
9	972	0.61	1.51	0.0405
10	1500	0.85	1.51	0.0405
11	2000	1.00	2.00	0.0405
12	2500	1.10	2.50	0.0675
13	3000	1.30	2.50	0.075
14	3500	1.30	3.00	0.081

15	4000	1.40	3.00	0.081
16	4500	1.50	3.50	0.081
17	5000	1.60	3.50	0.09
18	5500	1.70	3.5	0.1
19	6000	1.70	3.50	0.1
20	6500	1.80	4.00	0.1
21	7000	1.85	4.00	0.1
22	23.2	0.15	0.56	0.01
23	46.2	0.15	0.56	0.015
24	382	0.61	1.51	0.03
25	4500	1.50	2.10	0.081
26	5000	1.60	2.10	0.09
27	5500	1.70	2.32	0.1
28	6000	1.70	2.32	0.1
29	6500	1.80	2.30	0.1
30	7000	1.85	2.40	0.1

The burner diameters and ceiling heights for the simulations of Heskestad and Hamada's experiments (2), are the same as in the performed experiments. The range of HRRPUA (Heat release rate per unit area) produced from the burner area in these experiments is between 1000 kW/m^2 to 2050 kW/m^2. The burner diameter on the following experiments were set to a size were the HRRPUA corresponded with Heskestad and Hamada's HRRPUA at about 2000 kW/m^2, and did not exceed 3000 kW/m^2. It was also important to spread out the heat release area of the larger simulations to prevent jet fires, since it is diffusion flames that are of interest for the simulations of the flame extension length. The ceiling heights for the simulations outside 764 kW were set at a height were the flame extensions were deemed suitable for the intended purpose to determine the length of the flame extensions.

Simulations of the open flame height were also performed for each fire effect. The results from these simulations were used together with hand calculations using Heskestad's flame height correlation formula (1.2) to control the choice of grid cell size for the simulations. The results from these simulations could also be used in Heskestad and Hamada's flame extension formula (1.4) to calculate an expected value for the length of the flame extension expected from the simulations performed on this. The results for all the simulations are presented in chapter 4.

After simulations 1-7 were run, there were seen a deviation in the results of the flame extension length and flame height, compared to the calculated values using Equation(1.4) and Equation(1.2), in simulations 1, 2 and 5 as shown in Figure 16 and Figure 17. A resolution calculation of simulations 1-6 were then performed using Equation(1.8). It was found that the resolution of these three simulations where 5, 7 and 16. In the simulation on 764 kW which had a very good corresponding result, the resolution where 21. A resolution of 20 for a simulation is the resolutions used when validating Heskestad flame correlation formula in FDS (14). It was then decided that simulations 1, 2 and 5 should be run again with a new grid size that would give them a resolution of 20. It was also decided that all the simulations being run outside the experimental range of Heskestad and Hamada's experiments (2) should all have a resolution close to 20.

When the mean flame extension results from simulations 9 – 21 were analyzed, it showed a deviation of about 120 % for the simulations with an effect between 4500 – 7000 kW against the results from equation (1.4) shown in Figure 18. A first no reason for this could be found, until the results where closer studied. It was then discovered that the mean length of the flame extension was about the same length as half the burner size. From this the assumption that the energy in the flame extension was lower than 1% and that most of the energy where in the fire plume from the burner was made. It was then decided to lower the roof on these simulations to see if the amount of energy in the flame extension would increase and results could be made regarding the mean flame extension length on these fire effects.

3.2.1 Setup of 99 % heat release model in FDS

The method of finding the position where 99 % of the total heat release rate of the fire is was used to calculate the flame extension. This method was used when validating Heskestad flame height correlation formula as mentioned in chapter 2.4.

To be able to find the length of the flame extension under the ceiling, devices to measure heat release must be positioned in the FDS simulation. This can be done in two ways:

1. Placement of a device measuring the heat release rate for each timestep of the simulation in each grid cell of the simulation.
2. Placement of devices in the center of each grid cell in the centerline in x and y direction of the simulation. Measuring heat release rate per unit volume for each timestep of the simulation.

Method 2 was chosen because the amount of data method 1 would produce. An average simulation has 4920000 grid cells. If each of these had a device giving a measurement for each timestep of a 100s simulation, there would be $2.46\cdot10^{10}$ readings for one simulation. This amount of data requires a lot of computer processing power that were not available. Method 2 would produce 2000400 readings for a 100s simulation, giving a more reasonable amount of data. As mentioned above, in method 2 a device is place in the center of each grid cell in the centerline in x and y direction of the simulation. Each device will measure the heat release per unit volume in x and y direction. This is done for each cell by first multiplying the δ_x width of the cell in x direction of the grid cell the device is placed in, times the length of the cell in y direction, times the height z of the cell as shown in Figure 15. The length in y and z direction is from y_{min} to y_{max} and z_{min} to z_{max} for the simulation. The device then measures the heat release rate for this volume for each timestep. The devices placed in y direction in the center line, does the measurements the same way. The only difference is that it is done with a width of δ_y for the grid cell, and from x_{min} to x_{max} for the simulation. The measuring devices placed in a simulation can be seen as the small green circles in Figure 14.
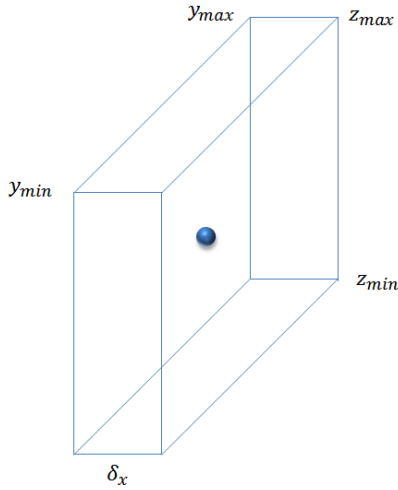
Figure 15 Sketch for measuring heat release rate per unit volume in a grid cell

The data given from the measuring devices allows the calculation of the flame extension length in –x, +x, -y and +y direction from the center of the fire.

3.3 Calculations

The calculations of flame extension length and flame height were performed using MATLAB.

The mean flame extension length and the mean flame height were calculated using scripts presented in Appendix D, and Appendix E. The scripts were an expansion of Randall McDermott's MATLAB script (17) used in validating Heskestad flame height correlation formula.

Both the flame extension and flame height was calculated as an average between 50 s and 100 s of the simulations. It in this time interval the fires were in a stable state giving the most representative readings.

3.3.1 Calculation of flame extension length performed in MATLAB

The flame extension was calculated in MATLAB using the script presented in Appendix D. This was done the following way:

1. The total heat release rate per unit volume was calculated in –x direction for each timestep, by adding each measured value from each device in each grid cell volume in the centerline from the center of the burner to x_{min}.
2. The measured values from the devices were then added, starting from the burner ending in the grid cell volume were the added value were 99 % of the total heat release per unit volume for that timestep.
3. The length for the flame extension length is then calculated using linear interpolation with the δ_x width of the cells included.
4. To find the mean flame extension length in –x direction for 50 to 100 s, the results for each flame extension length for each timestep from 50s to 100s, is added together and divided by the number of timesteps in this time period.
5. Steps 1 – 4 is then performed for +x, -y and +y direction.
6. The last step is to find the mean flame extension length for the simulation. This is done by adding the mean results from all the directions together and dividing by 4.

22

3.3.2 Calculation of model error

Calculations of the model error $\Delta_G(X)$ were made of the preformed simulations of mean flame extension length and mean flame height. The calculations were done using equation (1.5).In equation (1.5) the results from the simulations are set as *Z*, and the results from hand calculations using equation (1.4) for flame extension length, and equation (1.2) for flame height were set as *G(X)*. The results acquired from equation (1.5)are in meters [m].

A percentage calculation of the model error was also performed using equation(1.9). The values of *G(X)*, and *Z* used in equation (1.9) are the same as when the model error were calculated.

$$\Delta_{G_\%}\left(X\right) = \frac{G\left(X\right) - Z}{Z} \cdot 100 \tag{1.9}$$

The average percentage model error was calculated using equation (1.10):

$$\overline{\Delta_{G_\%}\left(X\right)} = \frac{1}{n}\sum_{i=1}^{n}\Delta_{G_\%}\left(X_i\right) \tag{1.10}$$

The standard percentage model error was calculated using equation (1.11):

$$s_{\Delta_{G_\%}\left(X\right)} = \sqrt{\frac{1}{n-1}\sum_{i=1}^{n}\left(\Delta_{G_\%}\left(X_i\right) - \overline{\Delta_{G_\%}\left(X_i\right)}\right)^2} \tag{1.11}$$

4 Results

In this chapter the results from the simulations will be presented. All the results from the performed simulations are available in Appendix F.

4.1 Results to improve simulations

The results presented here were used in the improvements of the simulations performed in FDS regarding the grid cell sizes, simulation resolution and adjustment of ceiling heights.
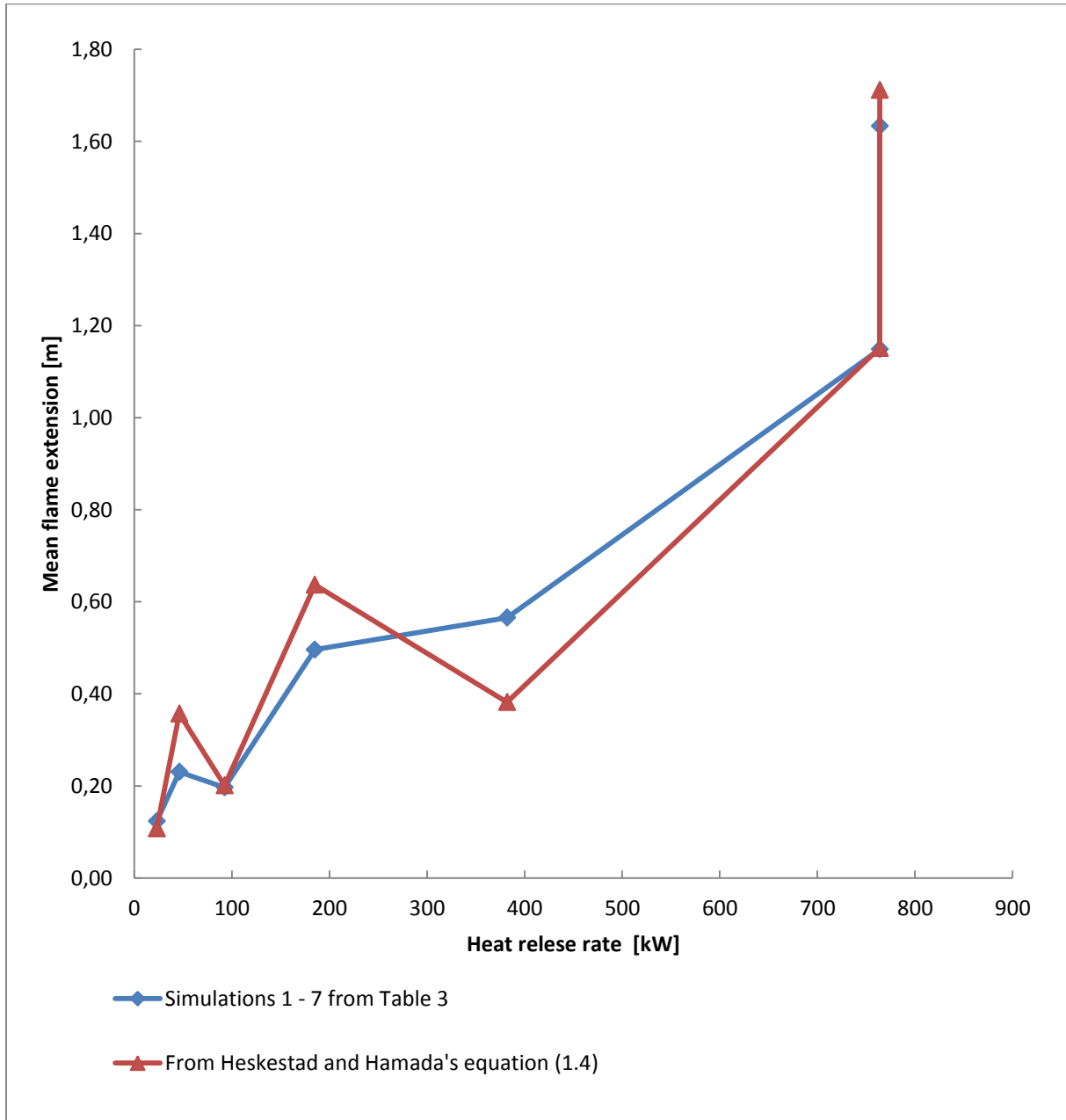
Figure 16 Flame extension length as a function of heat release rate results for simulations 1-7 from Table 3 and the results from Heskestad and Hamada's equation (1.4) as a function of the same heat release rates.

The mean flame extension for simulations 1 to 7 (see Table 3), and the calculated flame extension length using equation (1.4) are presented in Figure 16. As can be seen from the graph there are large deviations between the two curves at several heat release rates. The deviations shown in Figure 16

25

and Figure 17 resulted in the changes to the grid cell size for simulations 1, 2 and 5. This gave the simulations a resolution of 20 as presented in chapter 3.2. The results were also used in the decision to set the simulation resolution at 20 for the simulations with a heat release rate greater than 764 kW.
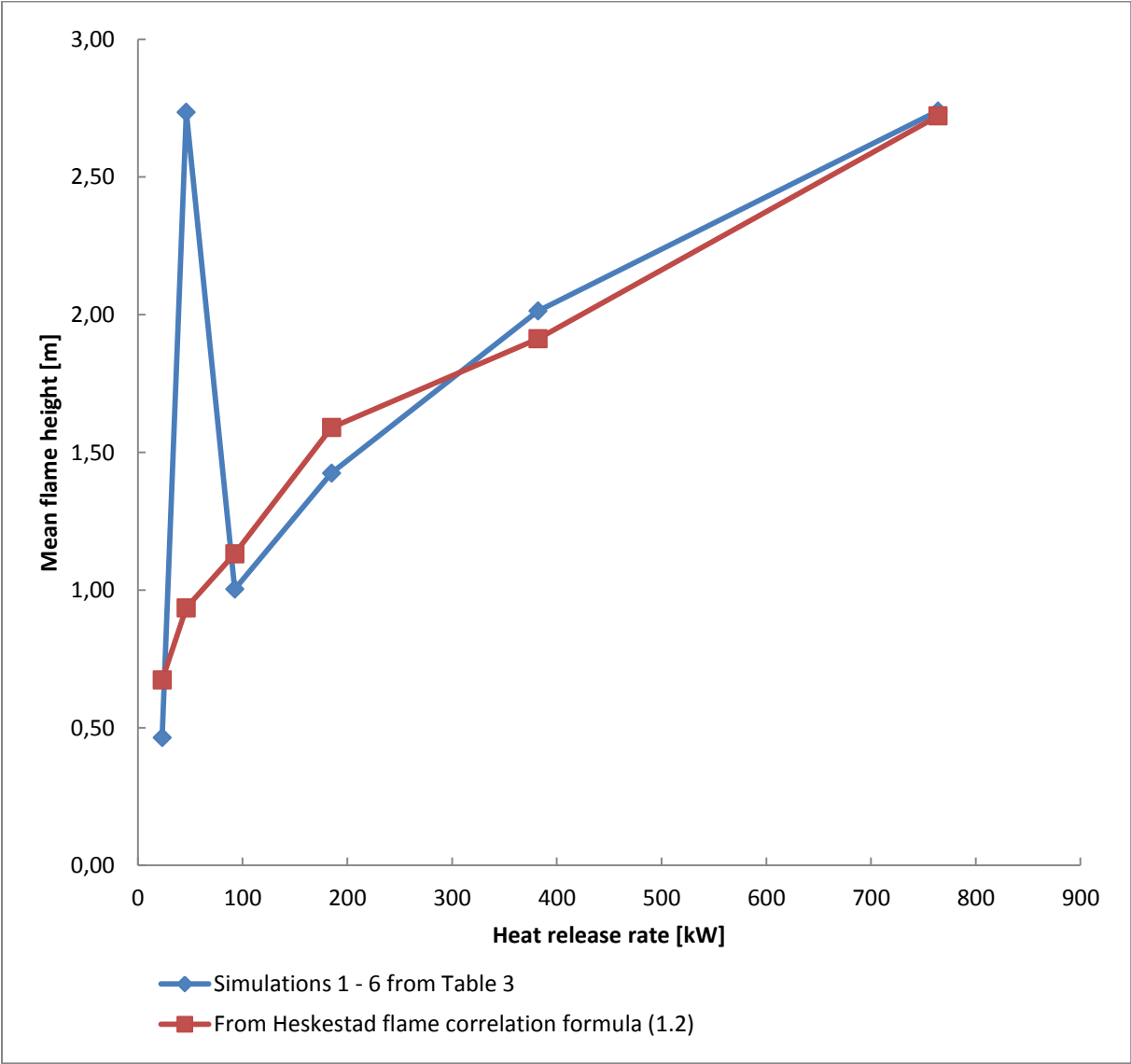
Figure 17 Mean flame height as a function of HRR for simulations 1 – 6 in Table 3 and the results from Heskestad flame correlation formula equation (1.2) as a function of the same heat release rates.

Figure 17 presents the mean flame height results from simulations with an heat release rate of 23.2 to 764 kW, against the results for these heat release rates calculated using Heskestad flame correlation formula equation (1.2). These effects are the same as the effects used in simulations 1 to 7. The two curves show two deviations in the flame height at 23.2 kW and 46.2 kW. These two deviations together with the deviations seen in Figure 16, led to the changes of grid cell size and simulation resolution presented in chapter 3.2.
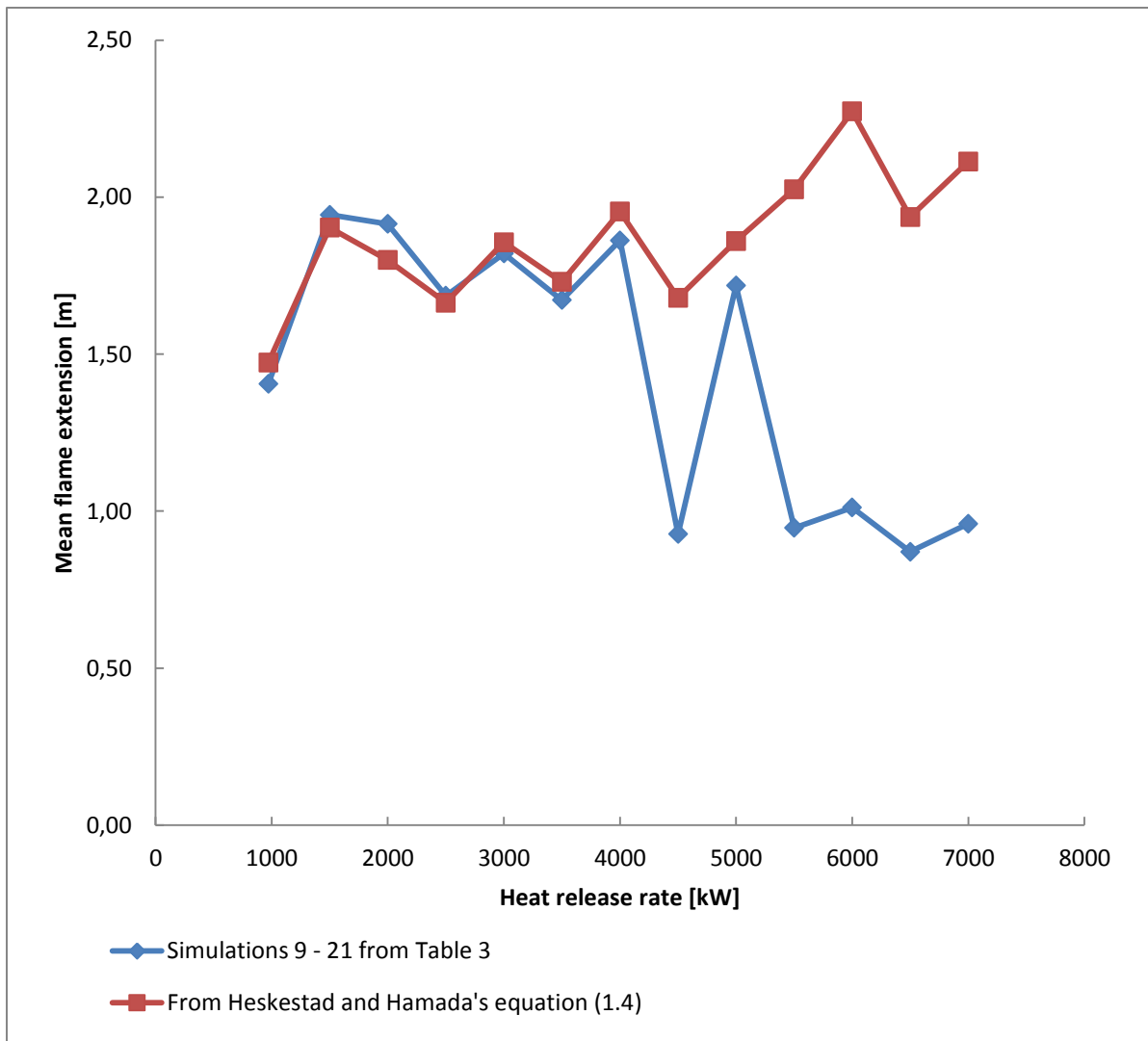
Figure 18 Mean flame extension length as a function of heat release rate for simulations 9-21 from Table 3 and the results from Heskestad and Hamada's equation (1.4)as a function of the same heat release rates.

Figure 18 shows the mean flame extension length for simulations 9 to 21 from Table 3 and the expected flame extension length for these effects using equation (1.4). Between 4500 kW and 7000 kW the simulated results for the mean flame extension varies significantly and irrationally. The difference between the simulated results and the calculations from equation (1.4) had an average deviation of 120 % at these heat release rates. The erratic behavior of the results is assumed to be related to the way the flame extension length is calculated, as discussed in chapter 3.2. Due to the low heat release rate in the flame extension it was decided that the ceiling height should be lowered for the simulations with heat release rates between 4500 kW and 7000 kW and that they should be repeated with an adjusted ceiling height.

4.2 Final simulation results

The figures in this chapter show the final results for flame extension and flame height. The simulated results come from the simulations with the finalized simulation resolution and adjusted ceiling height as presented in chapter 3.2. The calculated results are done using Heskestad and Hamada's flame extension equation (1.4) and Heskestad flame height correlation formula equation (1.2). The results for the percentage model error are available in Appendix G.
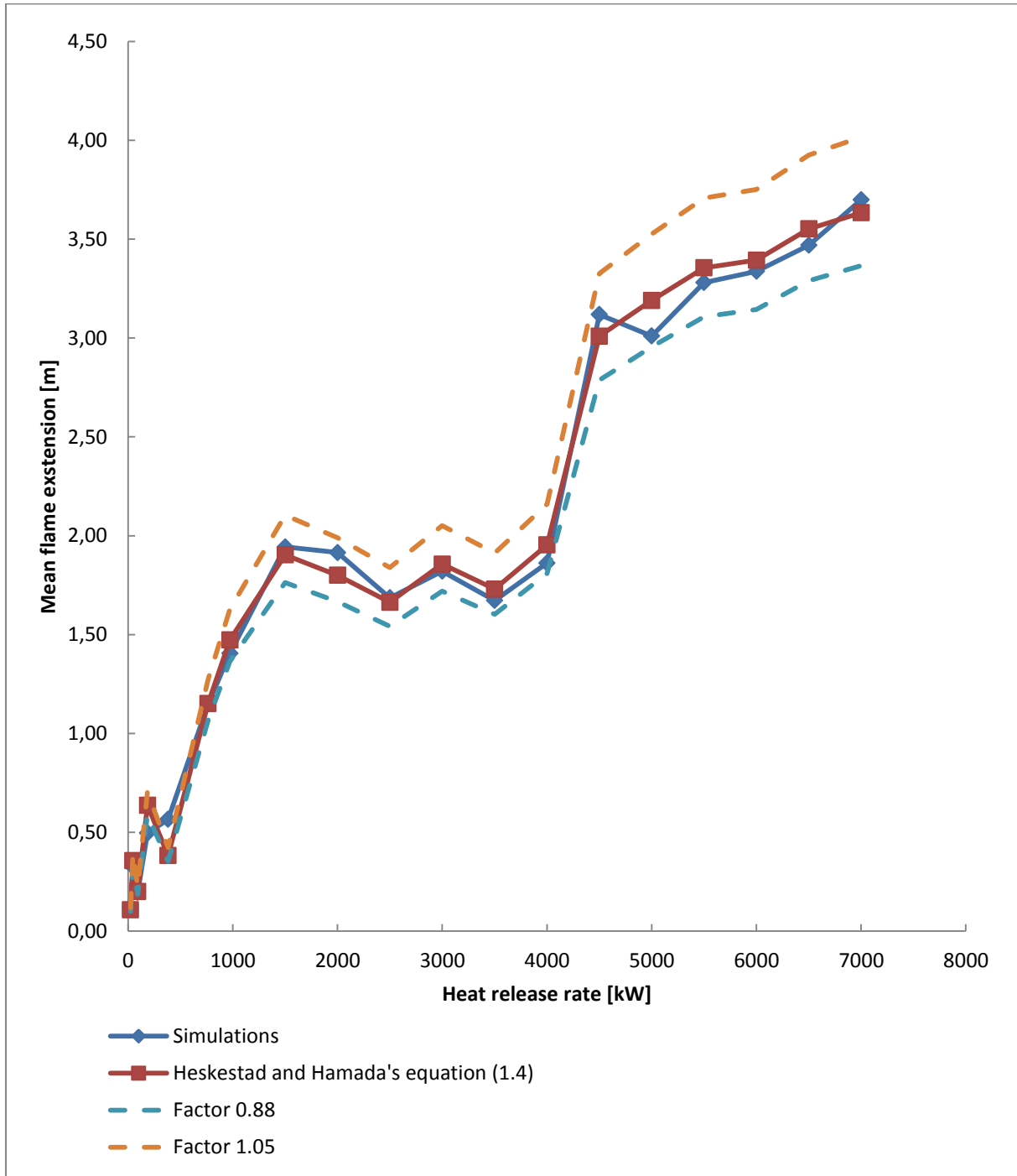
Figure 19 Mean flame extension as a function of heat release rate for the final simulations and Heskestad and Hamada's equation (1.4) as a function of the same heat release rates, with factor 0.88 and 1.05 used in equation 1.4 instead of 0.95

Figure 19 shows the curves of the final simulation results for the mean flame extension for the effects 23.2 kW to 7000 kW, the results from equation (1.4), calculated with the same input parameters that were used in the simulations. There are also added two dotted curves for the factors 0.88 and 1.05 used in equation (1.4) instead of 0.95. The interval between 0.88 and 1.05 was the amount of the free flame portion intercepted by the ceiling found by Heskestad and Hamada (2). The results in used in the curve for the mean flame extension for the simulations, are from the final simulations run (3, 4, 9 - 15, 22 – 30 from Table 3). As can be seen in Figure 19 the simulated results for the flame extension has the same overall shape as the results from equation (1.4). There are some simulated results that can be seen deviating from the calculated results, but most of the results are in between the upper and lower boundary of Heskestad and Hamada's estimation ($0.88(L-H)<r_f<1.05(L-H)$). The standard percentage model error (equation (1.12)) between simulated and calculated results (equation (1.4)) is ±10.80 %. The average percentage model error is 0.76 % when using equation (1.11).

The standard percentage model error of Heskestad and Hamada's seven performed experiments and the simulations for the same input quantities are ± 17.14 % with an average percentage model error of 0.34 %. Since it is only the model error of seven experiments used in these calculations it can be expected that the standard percentage model error is higher than the one calculated for the 20 simulations.

Heskestad and Hamada's flame extension equation (1.4) shows a standard percentage model error of ±3.48 % and an average model error of 0.98 % against the simulated results for heat release rates larger than 764 kW.
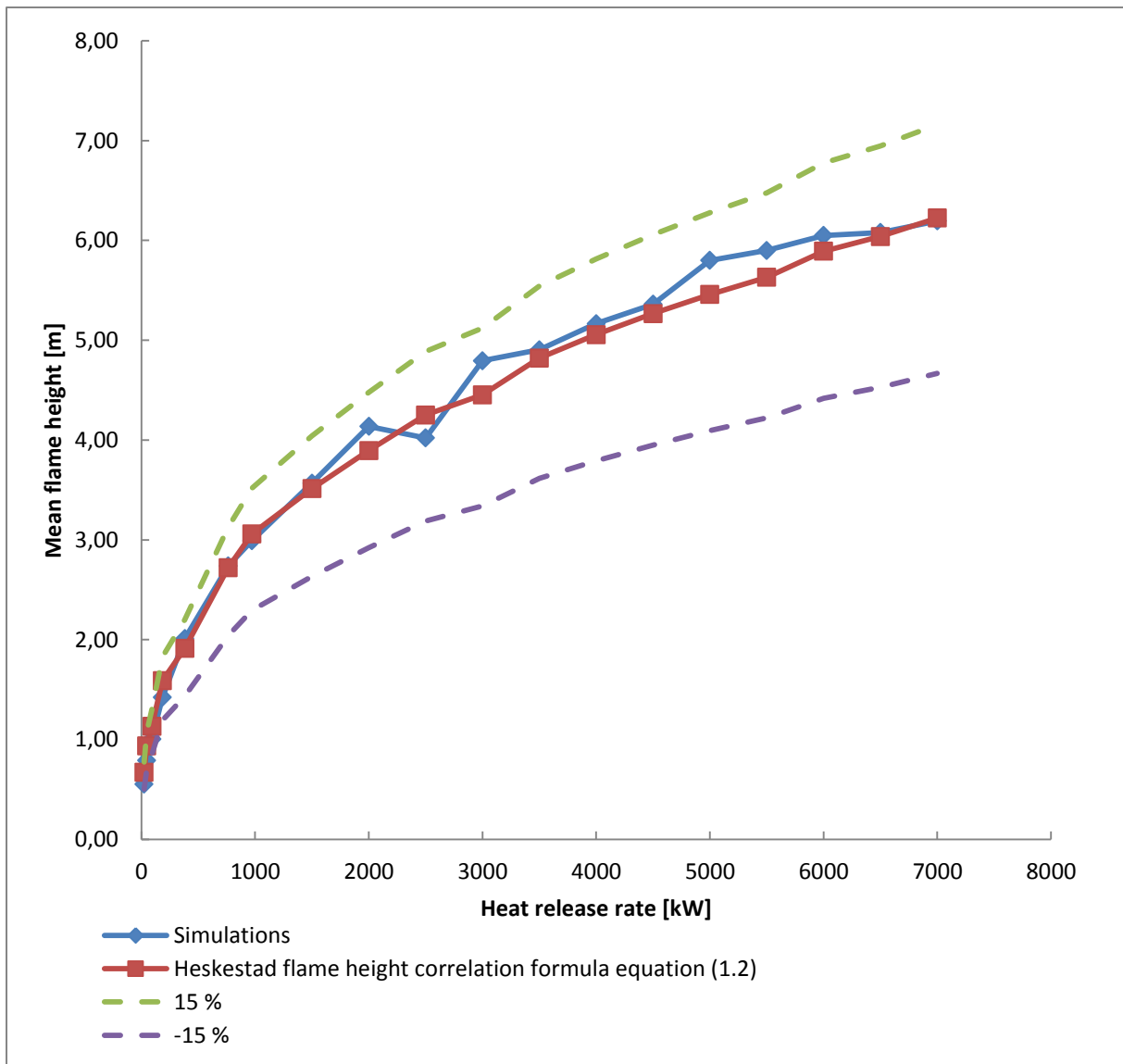
Figure 20 Mean flame height as a function of heat release rate from simulations with an heat release rate between 23.2 kW and 7000 kw, and Heskestad flame height correlation formula (1.2) as a function of the same heat release rates, with ±15 % curves of the calculated results from equation (1.2)

The mean flame height results from the simulations with an effect of 23.2 kW to 7000 kW, together with the results from Heskestad flame height correlation formula (1.2) for the same effects are presented in Figure 20. There are also two dotted curves in the graph, representing ±15 % of the flame height (L) as a result using equation (1.2). ±15 % was found as the uncertainty when Heskestad flame correlation formula was validated for FDS (14). As for Figure 19 the simulated results follow the overall shape of the calculated results using equation (1.2). There are some small deviations between the results in the two curves but nothing significant, and all the results are between the two stapled lines of ±15 % of the calculated values from equation (1.2). The standard percentage model error is ±8.13 % for the two curves. The average percentage model error is 1.75 %.
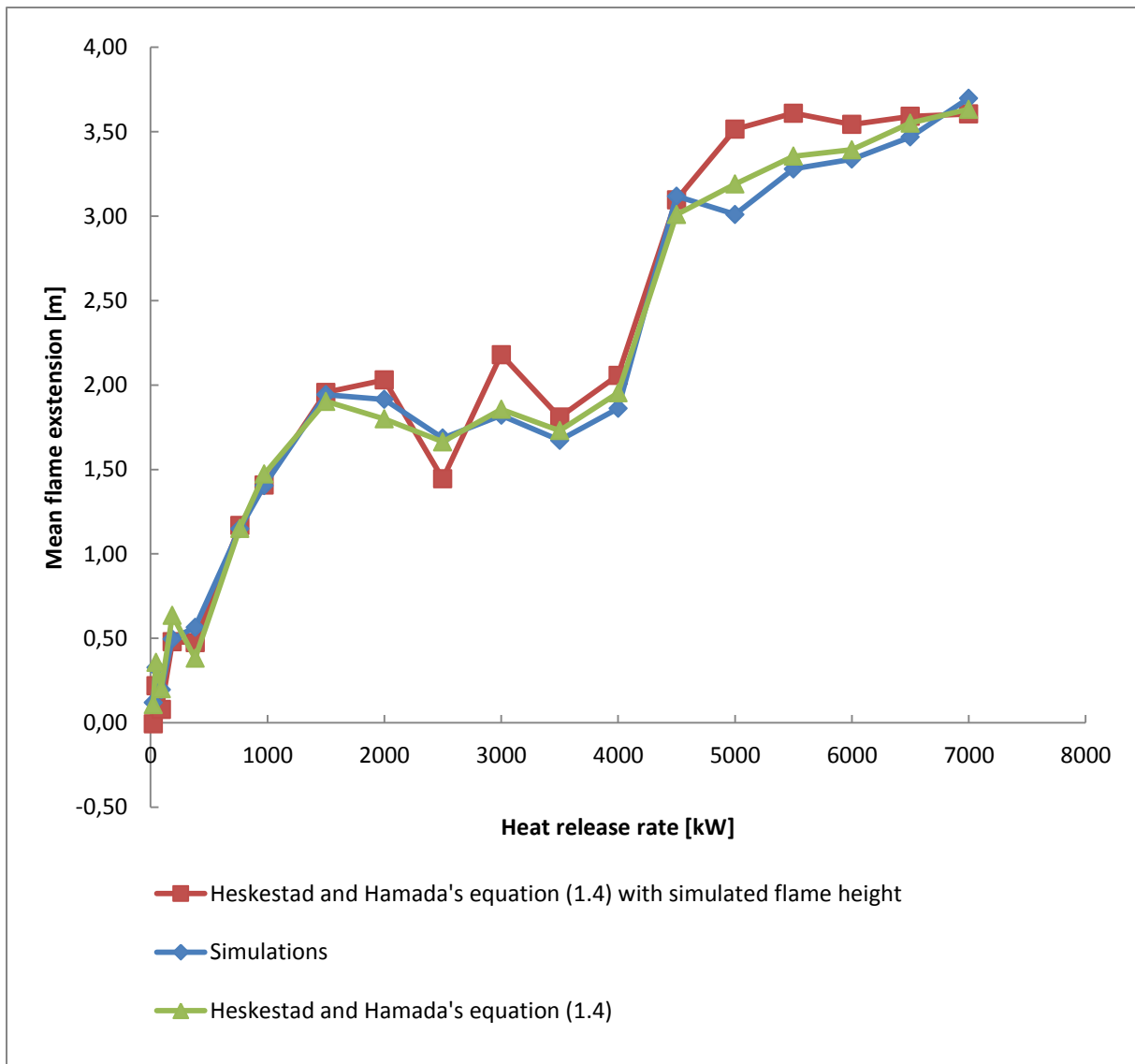
Figure 21 Mean flame extensions length as a function of heat release rate from performed simulations, the expected flame extension lengths calculated using equation (1.4) with the simulated flame heights as input values as a function of heat release rate, and flame extension as a function of heat release rate using Heskestad and Hamada's equation (1.4) with flame height from equation(1.2).

The curves in Figure 21 shows the results of the flame extension from the performed simulations, the expected flame extension calculated using equation(1.4) with the simulated flame height as a input quantity L in the equation, and the flame extension calculated using equation (1.4) with the flame height (L) calculated using equation (1.2) . As can be seen in the graph there are some differences between the curves. By comparing the differences in the curves in Figure 21 at 2000 kW, 2500 kW, 3000 kW and 5000 kW to 6500 kW, with the curves in Figure 19 and Figure 20, it can be seen that the simulated results at these points has some deviation from the calculated results. The standard percentage model error between the simulated results and the results from calculating the flame extension using equation (1.4) with the simulated flame height as input quantity is ± 28.33 %. The average percentage model error is -7.21 %. A negative percentage model error shows that the simulated results are larger than the calculated.

The standard percentage model error between Heskestad and Hamada's equation (1.4) with the flame height input quantity calculated using equation (1.2), and Heskestad and Hamada's equation (1.4) calculated with the simulated flame height as input quantity in the equation is ±29.26 %, with an average percentage model error of -7.55 %.

4.3 Sensitivity results

Table 4 Results from model sensitivity simulations

Simulation	Simulated mean flame extension length [m]	Expected flame extension length from equation (1.4)
1	1.1486	1.1495
2	1.1485	1.1495
3	1.1486	1.1495
4	1.1486	1.1495
5	1.1484	1.1495

A sensitivity analysis was conducted for a heat release rate of 764 kW.5 simulations where performed and the results are shown in Table 4. The results from the simulations show an extremely small variance in the results. There is a difference of $\pm 1 \cdot 10^{-4}$ m between the simulations from the mean result of 1.14854 m. This difference can come of numerical diffusion in the solutions of the Naiver-Stokes equations in FDS.

5   Discussion

5.1   Heskestad and Hamada's experiments

As presented in chapter 2.1.4 Heskestad and Hamada only performed seven experiments with a heat release rate between 23.2 and 764 kW when they developed equation (1.4) for calculating the flame extension length from a flame that impinges on a ceiling. There are no detailed results presented from these experiments in their article *"Ceiling jets of strong fire plumes"* (2), only that the factor of the free flame portion that were intercepted by the ceiling ranged from 0,88 to 1,05, with an average of 0,95 (2). Heskestad and Hamada does not specify in the article (2) which of the experiments gave what factor. The small number of experiments and the lack of details make comparative analysis difficult with respect on new experiments or simulations.

Since the flame extension equation (1.4) developed by Heskestad and Hamada is only based on seven experiments, the results the equation must be used with caution, and that until further experiments and validation work is performed on equation (1.4) it will only give rough uncertain estimates for the flame extension length under ceiling.

5.2   Simulation setup

The simulations performed in FDS where setup to resemble the experiments Heskestad and Hamada executed when developing equation (1.4) as closely as possible as presented in chapter 3.2. Some simplifications were made both to preserve processing power and to conform the simulations to the constraints in FDS. The simplification made to remove the table legs and the support of the roof should not have any impact on the simulations, but this can be discussed. One could argue that the roof supports and table legs could affect the air flow in the room, and thereby adding extra turbulence to the air flow for the fire, which in turn would affect the flame produced. The effect this would have on the fire depends on the size and placement of the ceiling supports and table legs. Heskestad and Hamada only mentions in their article (2) that the roof were hydraulically suspended, and that the burner were placed on a table. They do not mention the placement or size of either the suspension or table legs which makes them difficult to place in the simulations. The overall effect the ceiling support and table legs would have on the air flow is therefore hard to predict, but since the do not impact the fire directly the effect is seen as negligible. On the other hand, by removing the ceiling supports and table legs, processing power is saved when rendering the simulations. This decreases the simulations time for each simulation, allowing for faster results and more simulations to be run in a shorter time period.

There are two more simplifications made in the simulation setup in regard to Heskestad and Hamada's experiments (2) presented in chapter 3.2:

The first is the use of square burners instead of the circular burner Heskestad and Hamada used (2). This is done to conform the burner to the square grid of FDS. FDS has the ability to insert something circular in the simulation code. When the simulation is run however, FDS will rearrange this into squares again and numerically calculate the difference between the square and the circle. This can lead to numerical errors in the simulation and increase the uncertainty of the results. Since the square burner used in the simulations have the same HRRPUA as the circular burner used in the experiments, there should be no difference between the flames produced by the two types of burners, and there will be no numerical errors due to an eventual recalculation by FDS. The diameter

(*D*) of the burners in the simulations performed on heat release rates outside Heskestad and Hamada's experiment were all setup to give an HRRPUA that were in the same size as the HRRPUA of Heskestad and Hamada's experiments (2). It was also important that the flames produced by the burners were diffusion flames and not flames from a jet fire. Heskestad and Hamada's burners did not produce jet fires, and it was therefore important that the burners used in the experiment did no either.

The second simplification is the rearrangement of the roof from octagonal to a square roof. The shape of the roof the flame plume impinges on to produce a flame extension does not matter, as long as there are no confinements on the ceiling that will impact the behavior of the flame. The ceiling must however be wide enough for the flame extension, and not let any of the flame extension go outside its outmost edge. The flame extension will then turn upward, and its total length cannot be measured. The width of the roof is therefore increased beyond the 6,1 m used in the experiments for simulations where longer flame extension length then 2,0 m are anticipated.

As presented in chapter 3.2 the first simulation of 764 kW that was run had an grid dell size of 0.0405 m. The results from this simulation where so good compare to the expected result from equation (1.4), that the grid cell size was not changed when simulations 1 – 7 from Table 3 was simulated. This lead to the results presented in Figure 16 and Figure 17, where three simulations gave results that were questionable. After this a grid resolution calculation were made, and it was discovered that the resolution for the performed simulation where between 5 and 20. At this time the validation protocol for the validation of Heskestad flame correlation formula (14) for FDS were checked. In the protocol there had been performed simulations with three different resolutions 5, 10 and 20. Since the simulation with 764 kW heat release rate was shown to have a resolution of 21 and its results were shown to be good, and the validation were performed with a resolution of 20, it was decided that all the simulations performed on a heat release rate over 764 kW should have a grid cell size that gave the simulations a resolution of about 20. It was also decided that simulations 1, 2 and 5 from Table 3 should be rerun with new grid cell sizes.

It is important to remember to perform this calculation and to change the grid cell size accordingly when either changing the heat release rate $(\dot{Q})$ of the fire or the diameter (D) of the burner. Both these input parameters will have great effect on the simulations and will both affect the values of $\dot{Q}^*$ and D^* that are important when a simulation is setup. As it is shown in the results in Figure 19 and Figure 20, after the grid cell sizes where changed most of the results corresponded well to the calculated results from equation (1.4).

5.3   The choice of method

It is not easy to measure a flame length or flame height. When these measurements are performed in experiments it is often done visually by the luminosity of the flame. This is however not possible to do with simulations performed in FDS. FDS comes with a visualization program called Smokeview that is able to visualize the output of FDS. The visualization given by the program is only a rough rendering of the simulation as shown in Figure 22 and not good enough to use for exact measurements.
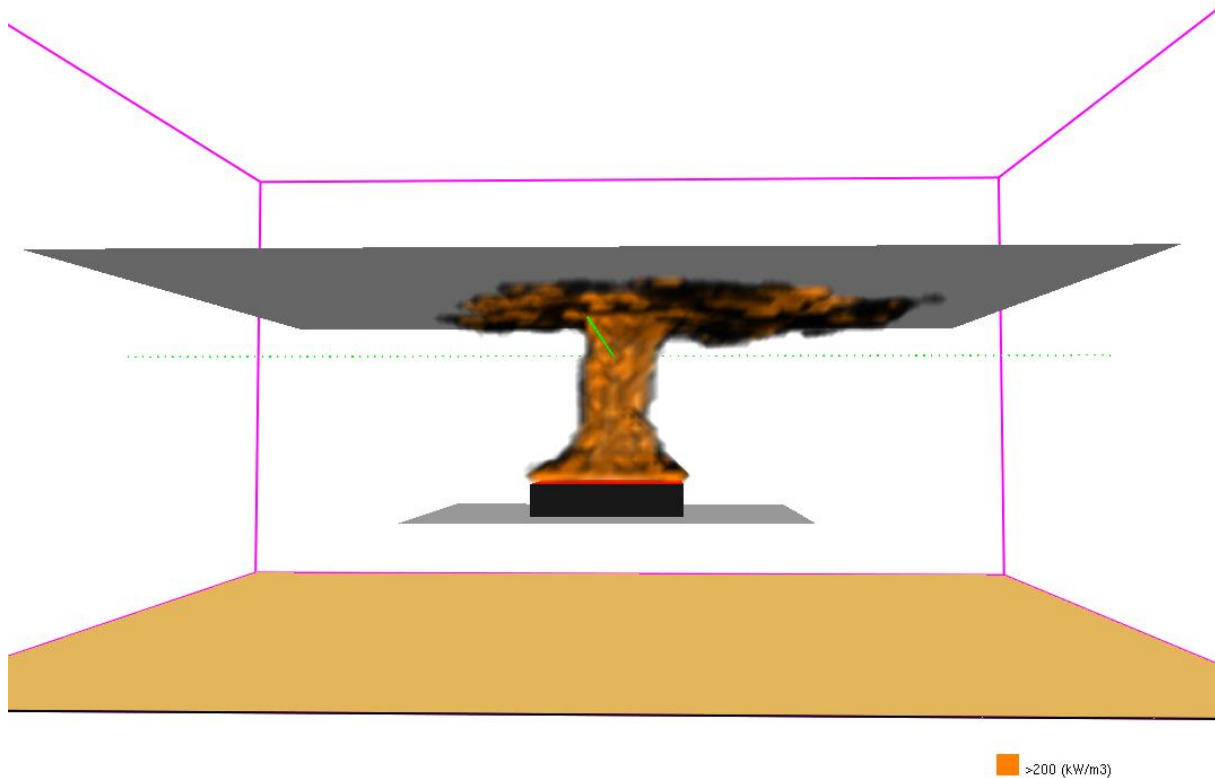
Figure 22 Screenshot from Smokeview showing the heat release per unit volume from a 7000 kW fire impinging on a ceiling

The method of finding the position of 99 % heat release rate from the fire in the simulation was used when calculating the flame extension. By using this method we would be able to calculate the flame extension length in four directions, and find a mean value for its length.

This method was however not without its limitations. When analyzing the data from simulations 9 – 21 from Table 3, something seemed to transpire with the mean flame extension for simulations 16 - 21 with an heat release rate between 4500 – 7000 kW as can be seen in Figure 18. How this could occur were at first unknown, until the data and results was more closely analyzed. It was the discovered that the mean flame extension for these simulations had the same approximate length as half the diameter of the burner, except for the simulation performed with an heat release rate of 5000 kW. Why the results from the 5000 kW simulation had a smaller deviation than the others are unknown. The roof height of this simulation was the same as for the simulations of 4500 kW, 5500 kW and 6000 kW and should have given the same kind of result as the other simulations. This will require further investigation in the future to find out why this occurred.

When the data from the simulations was analyzed, and the simulations were visually looked at using Smokeview, it showed that the simulations with a heat release rate between 4500 – 7000 kW had a flame extension from the fire. The reason why the flame extension calculations from the simulations did not include these flame extensions was still unclear. A more in depth analysis was performed on the calculations method, and it showed that the total heat release rate in the flame extension was less than 1 %. The calculation method finds the position where 99 % of the total heat release rate for the simulation is located, the flame extensions was not included in this calculation due to the low amount of the heat release rate in the extension.

This clearly shows a weakness with this method. To investigate this further, the ceiling height of the simulations were lowered, allowing for a larger amount of heat release rate in the flame extension. The results from these simulations (25-30 in Table 3) corresponded nicely with the results given by equation (1.4) as can be seen in Figure 19.

5.4   Uncertainty

When using models or simulations to describe experiments it is important to remember that these are only a simplified version of the event or system the model are representing or that are being simulated. When something is simplified from reality it will have uncertainties connected to it. The uncertainties regarding the simulations and Heskestad and Hamada's flame extension formula will be discussed in the following subheadings.

5.4.1   Simulation uncertainty

When performing simulations there are uncertainties associated with them. A simulation in FDS computes a solution of the Navier-Stokes equations for each grid cell volume. This computation involves an approximation of these equations, so it might not be correct to state that it solves the Navier-Stokes equations. The approximation performed by FDS includes a simplification of the physical assumptions regarding fires. This can for example be a simplification of the various techniques used for treating turbulence on a sub-grid scale (14). One of the most critical approximation FDS perform is the discretization of the governing equations. The discretization preformed can in turn lead to discretization errors in the calculations. How the approximations and in turn the discretization error will affect the uncertainty of a performed simulation is difficult to determine. A detailed convergence analysis can be performed to estimate the magnitude of the discretization error, but this will not give any direct answers to the size of the uncertainties (14). This is not the only area that affects the uncertainties of the simulations. In a CFD program there are a substantial amount of different subroutines used to make up a fire model. Each of these subroutines uses simplifications to solve their intended tasks. This lets more uncertainties be connected to a simulation. The more advanced the simulation is, the more subroutines are used, and this will in turn affect the uncertainty of the output result (14).

The simulations performed on Heskestad and Hamada's experiments (2), and on heat release rates outside their range of heat release rates can be viewed as simple simulations. Since the fuel used is propane gas was also used by Heskestad and Hamada (2). The use of this fuel in the simulation gives an advantage, since there is no need to use subroutines for pyrolysis modeling. In the simulations performed full heat transfer model is used on the ceiling. This subroutine allows for some uncertainties in the output result regarding the measurements of heat release rate in the grid cell volumes.

Uncertainties will always be connected to any simulation no matter how simple to simulate. How large the uncertainties are in the simulations performed here cannot be stated due to the complexity of the simulations despite that they can be seen as simple simulations. But it is important to remember that they are there when analyzing the results and drawing conclusions.

5.4.2   Uncertainty in the flame extension under ceiling formula

Equation (1.4) that Heskestad and Hamada developed for calculating the flame extension under a ceiling can be seen as a model. This since it calculates in mathematical terms a simplification of a specific situation that can occur when a fire plume impinges on a ceiling. By seeing equation (1.4) as

a model, the uncertainties connected to it can be discussed using the theory presented in chapter 2.2.2. By using this theory, the uncertainty in the model comes from two sources: input quantity (parameter) uncertainty and structural uncertainty. Each of these sources will here be discussed.

Input quantity (parameter) uncertainty is the uncertainty due to lack of knowledge about the input quantities X true values X_{true}. In equation (1.4) the input parameters are the open flame height L and the ceiling height (H). In most cases when this equation is used the ceiling height is known, and its value can often be seen as constant. The open flame height quantity (L) is however a quantity that is calculated from Heskestad flame height correlation formula (equation (1.2)). This formula will in turn have its own uncertainties connected to it that will affect the output results from its use. Since the output (L) is used as an input quantity in equation (1.4) it will increase the uncertainty of this equation by being an uncertain quantity in itself. There has been performed a lot of experiments on equation (1.2) over the years to assess the equations validity, and they show that the equation gives a good estimation of the mean open flame height (3), allowing for a more certain value of the quantity (L). This is good when using the results from equation (1.2) as an input quantity in equation (1.4) for the kind of fire scenarios investigated here. Here there is a constant fire with a known heat release rate $(\dot{Q})$, a known, constant fire diameter (D), and a known ceiling height (H). Both the heat release rate $(\dot{Q})$ and the fire diameter (D) are input quantities used in equation (1.2), since the true values in the simulations are known there will be no input quantity uncertainty from these impacting the input parameter (L) used in equation (1.2), and since the ceiling height (H) is known, both the true values of the input quantities used in equation (1.4) can be said to be known.

However, if equation (1.4) is used to calculate the flame extension length from a developing enclosed fire, the situation would be different. In such a scenario the fire starts small with a low heat release rate $(\dot{Q})$ and a small fire diameter (D). As the fire develops, these quantities will change with time. This change of the values of the input quantities $(\dot{Q})$ and (D) used in equation (1.2) over time, will produce an input quantity uncertainty in the equation since we then do not know their true values X_{true}. This in turn will give a more uncertain output result in the form of mean flame height (L), which is then used in equation (1.4) giving this equation an input quantity uncertainty from the quantity (L). So if equation (1.4) is used in scenarios such as these the results of the flame extension length under the ceiling would be uncertain due to the input quantity uncertainties in the equation.

Structural uncertainty is the uncertainty of the structure (G) of the model $G(X)$ when the true values X_{true} of the input quantities X used in the model are certain. In the case of equation (1.4) the structure of the equation was built on the results from seven experiments. The factor 0.95 in equation (1.4) is the amount of the free flame that impinged on the ceiling. The value 0.95 is an average value from the results of 0.88 – 1.05 in the performed experiments. The fact that the structure is built on such a small amount of data, the structure of the model must be seen as uncertain.

In the simulations performed for this thesis, we are certain of the true values X_{true} for the input quantities used in equation (1.4). Any uncertainties connected to the equation and the output result of the flame extension length from using equation (1.4) must therefore in this case be seen as structural uncertainties.

5.5 Results

In this chapter the results from the final simulations will be discussed. The results to improve simulations are discussed in chapter 5.2 and 5.3.

5.5.1 Flame extension results

When calculating the model error between the result given by Heskestad and Hamada's equation (1.4) seen as *G(X)* and the results from the simulations performed in FDS seen as *Z*, the resulting model error is has a unit in meters. This is relevant when looking at the model error between *G(X)* and *Z* for each heat release rate. Here there is one model error calculated for each heat release rate with corresponding ceiling height with results varying from -0.18 m to +0.18 m with an average of -0.02 m. The calculated flame extensions using equation (1.4) for heat release rates between 23.2 kW to 7000 kW varies between 0.12 m and 3.63 m. If the model error in meter were used to discuss and present these results they would not show how big the actual difference is between *G(X)* and *Z*. It was therefore decided to present and discuss the percentage difference of the model error between *G(X)* and *Z* and also to calculate the standard percentage model error between *G(X)* and *Z*.

It is also important to remember that simulations and their results are used to check the model error of a model. This will give an indication of how big the model error is, but any solid conclusions cannot be made regarding how well Heskestad and Hamada's equation (1.4) will calculate the flame extension from fires with flame that impinges on a ceiling.

It should also be mentioned that the code in FDS used in these simulations has not been altered to give the results discussed here. There is also no use of equation (1.4) when the mean flame extension was calculated in MATLAB by using the scripts presented in the appendix and the values given by the simulations.

As can been seen in Figure 19 the two curves have the same overall shape. The detailed results in Appendix F, for the results from using Heskestad and Hamada's equation (1.4), and the simulated results for the flame extension corresponds nicely. When the average percentage model error was calculated between the results it was surprising that it was only 0.8 % with a standard percentage model error of ±10.8 %. It was not expected that the simulated results would be as good as they are in regard to the calculated results using equation (1.4), and that they would correspond so well for fires with an heat release rate of more than 764 kW. The standard percentage model error of ±10.8 % clearly indicates that the flame extension formula (1.4) developed by Heskestad and Hamada can be used to calculate the flame extension of a fire that impinges on a ceiling.

There are however some results that needs mentioning. In the simulation with a heat release rate of 382 kW the percentage model error is -32.34 %. This heat release rate was simulated twice, once with a grid size of 0.0405 m and the second time with a grid cell size of 0.03 m. Why the result for the mean flame extension has not changed considerably between the two simulations is unknown. The grid cell size was also changed for the simulations with a heat release rate of 23.2 kW and 46.2 kW. When these simulations were run, the resulting flame extension results were more corresponding to the values expected using equation (1.4). Why this did not occur in the 382 kW simulation needs to be studied further. There is also a large percentage model error in the 185 kW simulation of 28.38 %. This equals a model error of 0.14 m for the calculated flame extension using equation (1.4) of 0.64 m. This was deemed an acceptable model error for this simulation, since the simulated flame extension

result of 0.50 m is still in the interval0.59 – 0.70 m given by equation (1.4) with the lower and upper boundary 0.88 and 1.05 found by Heskestad and Hamada.

5.5.2 Flame height results

When studying the flame height results from the simulations, and calculated results using Heskestad flame height correlation formula (1.2), for heat releases between 23.2 kW and 7000 kW (Figure 20 and in Appendix F), it can be seen that the two curves follow the same overall shape. The average percentage model error between the simulations and calculated results is 1.8 %, with a standard percentage model error of ±8.1 %. That the model error is so low is not surprising, since there has been performed a validation of Heskestad flame height correlation formula (1.2) in FDS. This validation gave an uncertainty (maximum variation) of ±15 % between the simulated results and the results from performed experiments. Here only two of the simulated results (23.2kW and 46.2 kW) are outside ±15 % of the calculated results using equation (1.2). These are the fires with the lowest heat release rate and smallest flame height, so any deviation between the calculated result and the simulated results will have a large percentage impact on the model error. The results for flame height were mostly used to check that the choice of grid cell sizes for the simulations was correct, and that the MATLAB model functioned correctly.

5.5.3 Flame extension for simulated flame heights

The three curves presented in Figure 21 shows the simulated mean flame extension and the flame extension calculated using equation (1.4) with the simulated flame height and the calculated flame height using equation (1.2) as an input parameter in equation (1.4). These three curves are meant to show the difference of the length of the flame extensions when using three different methods to calculate it.

As could be seen from the results regarding the flame extension discussed in chapter 5.5.1 the standard percentage model error between the two curves were only ±10.8 %. In that case the results from equation (1.4) was calculated using the mean flame height acquired from Heskestad flame height correlation formula (1.2). Here the results from equation (1.4) were also calculated using the simulated results for mean flame height that was discussed in chapter 5.5.2. The standard percentage model error between the two flame height curves were ±8.13 %. When the model error between the simulated mean flame extension and the flame extension calculated using equation (1.4) with the simulated flame height was analyzed it showed a standard percentage model error of ±28.3 %. If the same analysis is made between equation (1.4) with the simulated flame height and equation (1.4) with the calculated flame height using equation (1.2) the standard percentage model error is ±29.3 %.

Since the standard percentage model error is less when performing simulations of the mean flame extension and comparing the results with calculated results using Heskestad and Hamada's equation (1.4) with a flame height calculated using equation (1.2), then simulating the flame height and using it as an input quantity in equation (1.4), it is recommended to either simulate the flame extension in FDS or to calculate the flame extension using equation (1.4).

6 Conclusion

There are several conclusions that can be drawn from the simulations in FDS on flame extensions under ceiling, and the hand calculations using Heskestad and Hamada's flame extension formula (1.4) performed for this thesis.

In FDS the heat release per unit volume was measured for each simulation. These results was then used to calculate the position were 99 % of the heat release rate was in the simulation with the help of MATLAB. The calculated results from the simulation compared to the results from equation (1.4) shows that the 99 % model can be used to find the mean flame extension from simulations in FDS. This model has its limitations and uncertainties when it comes to flame extensions with a low percentage of the total heat release rate. If the total heat release rate in the flame extension is below 1 % of the total heat release rate from the fire, the result from the 99 % model will be inaccurate due to the calculation method used. This model functions for the simulations performed for this report, but further work is needed to develop this model and look at alternative methods for calculating the mean flame extension from simulations performed in FDS.

By letting the simulated results regarding the mean flame extension represent the observed quantity *Z*, and the results calculated using Heskestad and Hamada's equation (1.4) be represented as *G(X)*, the model error for Heskestad and Hamada's flame extension formula (1.4) could be calculated. The results from these calculations were surprisingly good. The standard average model error for the final 20 simulations is ±10.8 % with an average percentage model error of 0.8 %. However, it is important to remember that a model (simulations in FDS) is used to find the model error of another model. Since there are uncertainties connected to any simulation performed in a CFD-program, the results from the simulations cannot be seen as 100 % accurate. There are also some uncertainties regarding the formula developed by Heskestad and Hamada, since the factor of 0.95 used in the formula came from only seven experiments, with results spanning between 0.88 and 1.05. In regard to the uncertainties connected to the two models used, a definite conclusion about the model error and accuracy of Heskestad and Hamada's formula cannot be made. It can however be said that the results here gives an indication that Heskestad and Hamada's formula can be used for fires with an heat release rate between 23.2 kW and 7000 kW. To be able to make a more definite conclusion more real experiments on flame extensions is needed with a heat release rate higher than 764 kW. It should also be performed more simulations on flame extensions in FDS, with a narrower interval between the heat release rates used in the simulations, to improve the standard deviation of the model error between the simulated results and the results from equation (1.4).

A calculation was also performed of the model error between the simulated flame extension and a calculated flame extension using the simulated flame height results as an input quantity in equation (1.4), and a calculation using equation (1.4) with a flame height calculated from equation (1.2). These results showed that the standard percentage model error is larger if the flame extension is calculated using the simulated flame height in equation (1.4), than using the flame height calculated from Heskestad flame correlation formula (1.2) in equation (1.4). This shows, that if the flame extension is of interest from a flame that impinges on a ceiling, it is better to set up a full simulation and use the 99 % heat release model or calculating the flame extension with equation (1.4) and using a flame height calculated using equation (1.2) as an input parameter.

7 Further work

As presented in both the discussion and conclusion, this thesis has given several ideas for further work in the future.

In the simulations performed for this thesis the 99 % heat release rate model was used to find the flame extension. As has been presented this model needs some refinement work regarding flame extensions with a low percentage of the total heat release rate. If this model is proven not to be able to handle that kind of scenarios, another method needs to be developed for future use in FDS.

There were also some problems with the 382 kW and 5000 kW simulations performed. These simulations need to be investigated further, to find out why they did not produce the expected results.

It also needs to be performed more simulations with a narrower interval between the heat release rates in the simulations. This will give more results to compare with results from Heskestad and Hamada's flame extension formula and give a more reliable standard percentage model error.

The most important work in the future is however to perform more real experiments on flame extensions. These experiments would help to continue the development of Heskestad and Hamada's flame extension formula. The results from the experiments could also be used together with simulation results to validate Heskestad and Hamada's flame extension formula for FDS.

References

1. **You, H.Z. and Faeth, G.M.** *An investigation of fire impingement on a horizontal ceiling.* Washington D.C. : National Bureau of Standards, 1981. NBS-GCR-81-304.

2. **Heskestad, G and Hamada, T.** Ceiling jets of strong fire plumes. *Fire safety journal.* 21, 1993, pp. 69-82.

3. **Karlsson, Björn and Quintiere, James, G.** *Ebclosure Fire Dynamics.* Boca Raton : CRC Press LLC, 2000. 0-8493-1300-7.

4. **Hagen, Bjarne Christian.** *Grunnleggende brannteknikk.* [Haugesund] : Bjarne Christian Hagen, 2004.

5. **Griffiths, J.F and Barnard, J.A.** *Flame and combustion.* Glasgow : Blackie Academic Proffesional, 1995.

6. **Ding, H and Quintiere, G.** An integral model for turbulent flame radial lengths under ceiling. *Fire safety journal.* 52, 2012, pp. 25-33.

7. **Ingason, H, Zhen Li, Y and Lönnemark, A.** *Tunnel fire dynamics.* New York : Springer, 2015. ISBN 978-1-4939-2198-0.

8. **Stevenson, Angus, [ed.].** *Oxford Dictionary of English.* Oxford : Oxford University Press, 2015.

9. **Aven, T and Nilsen, T.** Models and model uncertainty in the context of risk analysis. *Reliability engineering & system safety.* 79, March 1, 2003, 3, pp. 309-317.

10. **Aven, Terje and Zio, Enrico.** Model Output Uncertainty in Risk Assessment. *International Journal of Performability Engineering.* 9, September 2013, 5, pp. 475-486.

11. **Loucks, D.P. and van Beek, E.** *Water resources sytems planning and management.* Paris : Ages Arti Grafiche, 2005. ISBN 92-3-103998-9.

12. **Frey, H.C and Patil, S.R.** Identification and rewiew of sensitivity analysis methods. *Risk Analysis.* 22, 2002, 3.

13. **Borg, Audun and Njå, Ove.** Concept of validation in performance-based fire safety engineering. *Safety Science.* 52, 2013, pp. 57-64.

14. **McGrattan, Kevin, et al., et al.** *Fire Dynamics Simulator Technical Reference Guide Volume:3 Validation.* s.l. : U.S. Department of Commerce, 2015.

15. —. *Fire Dynamics Simulator User's Guide.* s.l. : U.S. Department of Commerce, 2015.

16. **Chapman, B, Jost, G and van der Pas, R.** *Using OpenMP - Portable Shared Memory Parallel Programming.* Massachusetts : MIT Press, 2007.

17. **McDermott, R.** Fire Dynamics Simulator and Smokeview. [Online] 4 2, 2011. [Cited: 11 19, 2015.] http://fds-smv.googlecode.com/svn/trunk/FDS/trunk/Utilities/Matlab/scripts/flame_height.m.

18. **DiNenno, Philip J, [ed.].** *The SFPE Hanbbok of fire protection engineering.* Quincy : NFPA, 2008. p. Chapter 1.

8 Appendix

8.1 Appendix A

Material properties used in FDS simulations

Marinite I

Thermal conductivity (24 - 538°C)	0,12 W/mK
Specific heat capacity at 425°C	1,424 J/gK
Density	737 kg/m^3

Asbestos-cement board

Thermal conductivity	0,744 W/mK
Specific heat capacity	0,84 kJ/kgK
Density	1400 kg/m^3

Plywood

Thermal conductivity	0,12 W/mK
Specific heat capacity	1,215 kJ/kgK
Density	545 kg/m^3

8.1 Appendix A

Material properties used in FDS simulations

8.2 Appendix B

Setup in FDS of 764 kW simulation.

/ Setup simulation master thesis

&HEAD CHID= 'full-100s-764kw', TITLE= 'Setup' /

&TIME T_END= 100, / Length of simulation, 0 for setup

/***************** COMPUTATIONAL GRID ***************************************

&MESH IJK= 100, 100, 62, XB= -4.05, 4.05, -4.05, 4.05, -1.42, 3.602 / 4 920 000 cells

/********************* Obstructions **

/Gulv

&OBST XB= -2.44, 2.44, -2.44, 2.44, 0.0, -0.0095, SURF_ID= 'FLOOR1'/ Cement-asbestos

&OBST XB= -2.44, 2.44, -2.44, 2.44, -0.0095, -0.0345, SURF_ID= 'FLOOR2'/ Plywood

/Burner

&OBST XB= -0.305, 0.305, -0.305, 0.305, 0.0, 0.3843, SURF_ID= 'BURNER'/ Burner

/Tak

&OBST XB= -3.05, 3.05, -3.05, 3.05, 1.8943, 1.907, SURF_ID= 'ROOF1'/ Marinite XL

&OBST XB= -3.05, 3.05, -3.05, 3.05, 1.907, 1.932, SURF_ID= 'ROOF2'/ Steel channel lattice

/******************* Passive ventilations openings: *************************

&VENT XB= -4.05, 4.05, -4.05, -4.05, -1.42, 3.602, SURF_ID='OPEN',/ Ventilation front

&VENT XB= -4.05, 4.05, 4.05, 4.05, -1.42, 3.602 , SURF_ID='OPEN',/ Ventilation back

&VENT XB= -4.05, -4.05, -4.05, 4.05, -1.42, 3.602, SURF_ID='OPEN',/ Ventilation left side

&VENT XB= 4.05, 4.05, -4.05, 4.05, -1.42, 3.602, SURF_ID='OPEN',/ Ventilation right side

&VENT XB=-4.05, 4.05, -4.05, 4.05, 3.602, 3.602, SURF_ID='OPEN',/-1.42 Ventilation top

/******************* Fire **

&REAC ID =   'PROPANE'

              FUEL='PROPANE'

              SOOT_YIELD = 0.01

C = 3.

                    H = 8.

                    HEAT_OF_COMBUSTION = 46460.

                    IDEAL = .TRUE. /

&SURF ID='FIRE1',HRRPUA=2053.211502, COLOR='RED', /

&VENT XB= -0.305, 0.305, -0.305, 0.305, 0.3843, 0.3843, SURF_ID= 'FIRE1',/ Constant 764 kW fire

/********************* Output ***

&DUMP DT_RESTART=10, DT_SLCF=0.5, DT_DEVC=0.02, DT_ISOF=10, DT_PL3D=20, DT_BNDF=1.,
PLOT3D_QUANTITY(5)='VISIBILITY'

/   DT_RESTART=10:   Backup for hvert 10 sek, således at hvis simuleringen går ned kan
startes herfra.

/   DT_SLCF=0.5:   Time between each picture in slice file

/   DT_DEVC=0.02: Time between each output of devices.

/   DT_ISOF=10:   Time between each picture of Isosurfaces, billeder.

/   DT_PL3D=20:   Time between each picture in 3D plotfiles.

/   DT_BNDF=1:   Time between each picture i boundaryfiles.

/   PLOT3D_QUANTITY(5)='visibility' Changesdefault 3D plotfiles from HHR to visibility.

&SLCF PBY= 0.0, QUANTITY='VELOCITY', /

&SLCF PBY= 0.0, QUANTITY='TEMPERATURE', /

&SLCF PBY= 0.0, QUANTITY='HRRPUV', /

&SLCF PBX= 0.0, QUANTITY='TEMPERATURE',VECTOR=.TRUE., /

&ISOF QUANTITY='TEMPERATURE', VALUE(1)=540, VALUE(2)=550,/

&BNDF QUANTITY='RADIATIVE HEAT FLUX', /

&BNDF QUANTITY='WALL TEMPERATURE', /

/******************* DEVICES ***

D

&DEVC ID='hrrpuv_x1', XB=-4.05,-3.969,-4.05,4.05,-1.42,3.602, QUANTITY='HRR'/

&DEVC ID='hrrpuv_x2', XB=-3.969,-3.888,-4.05,4.05,-1.42,3.602, QUANTITY='HRR'/

&DEVC ID='hrrpuv_x3', XB=-3.888,-3.807,-4.05,4.05,-1.42,3.602, QUANTITY='HRR'/

&DEVC ID='hrrpuv_x4', XB=-3.807,-3.726,-4.05,4.05,-1.42,3.602, QUANTITY='HRR'/

&DEVC ID='hrrpuv_x5', XB=-3.726,-3.645,-4.05,4.05,-1.42,3.602, QUANTITY='HRR'/

&DEVC ID='hrrpuv_x6', XB=-3.645,-3.564,-4.05,4.05,-1.42,3.602, QUANTITY='HRR'/

&DEVC ID='hrrpuv_x7', XB=-3.564,-3.483,-4.05,4.05,-1.42,3.602, QUANTITY='HRR'/

&DEVC ID='hrrpuv_x8', XB=-3.483,-3.402,-4.05,4.05,-1.42,3.602, QUANTITY='HRR'/

&DEVC ID='hrrpuv_x9', XB=-3.402,-3.321,-4.05,4.05,-1.42,3.602, QUANTITY='HRR'/

&DEVC ID='hrrpuv_x10', XB=-3.321,-3.24,-4.05,4.05,-1.42,3.602, QUANTITY='HRR'/

&DEVC ID='hrrpuv_x11', XB=-3.24,-3.159,-4.05,4.05,-1.42,3.602, QUANTITY='HRR'/

&DEVC ID='hrrpuv_x12', XB=-3.159,-3.078,-4.05,4.05,-1.42,3.602, QUANTITY='HRR'/

&DEVC ID='hrrpuv_x13', XB=-3.078,-2.997,-4.05,4.05,-1.42,3.602, QUANTITY='HRR'/

&DEVC ID='hrrpuv_x14', XB=-2.997,-2.916,-4.05,4.05,-1.42,3.602, QUANTITY='HRR'/

&DEVC ID='hrrpuv_x15', XB=-2.916,-2.835,-4.05,4.05,-1.42,3.602, QUANTITY='HRR'/

&DEVC ID='hrrpuv_x16', XB=-2.835,-2.754,-4.05,4.05,-1.42,3.602, QUANTITY='HRR'/

&DEVC ID='hrrpuv_x17', XB=-2.754,-2.673,-4.05,4.05,-1.42,3.602, QUANTITY='HRR'/

&DEVC ID='hrrpuv_x18', XB=-2.673,-2.592,-4.05,4.05,-1.42,3.602, QUANTITY='HRR'/

&DEVC ID='hrrpuv_x19', XB=-2.592,-2.511,-4.05,4.05,-1.42,3.602, QUANTITY='HRR'/

&DEVC ID='hrrpuv_x20', XB=-2.511,-2.43,-4.05,4.05,-1.42,3.602, QUANTITY='HRR'/

&DEVC ID='hrrpuv_x21', XB=-2.43,-2.349,-4.05,4.05,-1.42,3.602, QUANTITY='HRR'/

&DEVC ID='hrrpuv_x22', XB=-2.349,-2.268,-4.05,4.05,-1.42,3.602, QUANTITY='HRR'/

&DEVC ID='hrrpuv_x23', XB=-2.268,-2.187,-4.05,4.05,-1.42,3.602, QUANTITY='HRR'/

&DEVC ID='hrrpuv_x24', XB=-2.187,-2.106,-4.05,4.05,-1.42,3.602, QUANTITY='HRR'/

&DEVC ID='hrrpuv_x25', XB=-2.106,-2.025,-4.05,4.05,-1.42,3.602, QUANTITY='HRR'/

&DEVC ID='hrrpuv_x26', XB=-2.025,-1.944,-4.05,4.05,-1.42,3.602, QUANTITY='HRR'/

&DEVC ID='hrrpuv_x27', XB=-1.944,-1.863,-4.05,4.05,-1.42,3.602, QUANTITY='HRR'/

&DEVC ID='hrrpuv_x28', XB=-1.863,-1.782,-4.05,4.05,-1.42,3.602, QUANTITY='HRR'/

&DEVC ID='hrrpuv_x29', XB=-1.782,-1.701,-4.05,4.05,-1.42,3.602, QUANTITY='HRR'/

&DEVC ID='hrrpuv_x30', XB=-1.701,-1.62,-4.05,4.05,-1.42,3.602, QUANTITY='HRR'/

&DEVC ID='hrrpuv_x31', XB=-1.62,-1.539,-4.05,4.05,-1.42,3.602, QUANTITY='HRR'/

&DEVC ID='hrrpuv_x32', XB=-1.539,-1.458,-4.05,4.05,-1.42,3.602, QUANTITY='HRR'/

&DEVC ID='hrrpuv_x33', XB=-1.458,-1.377,-4.05,4.05,-1.42,3.602, QUANTITY='HRR'/

&DEVC ID='hrrpuv_x34', XB=-1.377,-1.296,-4.05,4.05,-1.42,3.602, QUANTITY='HRR'/

&DEVC ID='hrrpuv_x35', XB=-1.296,-1.215,-4.05,4.05,-1.42,3.602, QUANTITY='HRR'/

&DEVC ID='hrrpuv_x36', XB=-1.215,-1.134,-4.05,4.05,-1.42,3.602, QUANTITY='HRR'/

&DEVC ID='hrrpuv_x37', XB=-1.134,-1.053,-4.05,4.05,-1.42,3.602, QUANTITY='HRR'/

&DEVC ID='hrrpuv_x38', XB=-1.053,-0.972,-4.05,4.05,-1.42,3.602, QUANTITY='HRR'/

&DEVC ID='hrrpuv_x39', XB=-0.972,-0.891,-4.05,4.05,-1.42,3.602, QUANTITY='HRR'/

&DEVC ID='hrrpuv_x40', XB=-0.891,-0.81,-4.05,4.05,-1.42,3.602, QUANTITY='HRR'/

&DEVC ID='hrrpuv_x41', XB=-0.81,-0.729,-4.05,4.05,-1.42,3.602, QUANTITY='HRR'/

&DEVC ID='hrrpuv_x42', XB=-0.729,-0.648,-4.05,4.05,-1.42,3.602, QUANTITY='HRR'/

&DEVC ID='hrrpuv_x43', XB=-0.648,-0.567,-4.05,4.05,-1.42,3.602, QUANTITY='HRR'/

&DEVC ID='hrrpuv_x44', XB=-0.567,-0.486,-4.05,4.05,-1.42,3.602, QUANTITY='HRR'/

&DEVC ID='hrrpuv_x45', XB=-0.486,-0.405,-4.05,4.05,-1.42,3.602, QUANTITY='HRR'/

&DEVC ID='hrrpuv_x46', XB=-0.405,-0.324,-4.05,4.05,-1.42,3.602, QUANTITY='HRR'/

&DEVC ID='hrrpuv_x47', XB=-0.324,-0.243,-4.05,4.05,-1.42,3.602, QUANTITY='HRR'/

&DEVC ID='hrrpuv_x48', XB=-0.243,-0.162,-4.05,4.05,-1.42,3.602, QUANTITY='HRR'/

&DEVC ID='hrrpuv_x49', XB=-0.162,-0.081,-4.05,4.05,-1.42,3.602, QUANTITY='HRR'/

&DEVC ID='hrrpuv_x50', XB=-0.081,0.0,-4.05,4.05,-1.42,3.602, QUANTITY='HRR'/

&DEVC ID='hrrpuv_x51', XB=0.0,0.081,-4.05,4.05,-1.42,3.602, QUANTITY='HRR'/

&DEVC ID='hrrpuv_x52', XB=0.081,0.162,-4.05,4.05,-1.42,3.602, QUANTITY='HRR'/

&DEVC ID='hrrpuv_x53', XB=0.162,0.243,-4.05,4.05,-1.42,3.602, QUANTITY='HRR'/

&DEVC ID='hrrpuv_x54', XB=0.243,0.324,-4.05,4.05,-1.42,3.602, QUANTITY='HRR'/

&DEVC ID='hrrpuv_x55', XB=0.324,0.405,-4.05,4.05,-1.42,3.602, QUANTITY='HRR'/

&DEVC ID='hrrpuv_x56', XB=0.405,0.486,-4.05,4.05,-1.42,3.602, QUANTITY='HRR'/

&DEVC ID='hrrpuv_x57', XB=0.486,0.567,-4.05,4.05,-1.42,3.602, QUANTITY='HRR'/

&DEVC ID='hrrpuv_x58', XB=0.567,0.648,-4.05,4.05,-1.42,3.602, QUANTITY='HRR'/

&DEVC ID='hrrpuv_x59', XB=0.648,0.729,-4.05,4.05,-1.42,3.602, QUANTITY='HRR'/

&DEVC ID='hrrpuv_x60', XB=0.729,0.81,-4.05,4.05,-1.42,3.602, QUANTITY='HRR'/

&DEVC ID='hrrpuv_x61', XB=0.81,0.891,-4.05,4.05,-1.42,3.602, QUANTITY='HRR'/

&DEVC ID='hrrpuv_x62', XB=0.891,0.972,-4.05,4.05,-1.42,3.602, QUANTITY='HRR'/

&DEVC ID='hrrpuv_x63', XB=0.972,1.053,-4.05,4.05,-1.42,3.602, QUANTITY='HRR'/

&DEVC ID='hrrpuv_x64', XB=1.053,1.134,-4.05,4.05,-1.42,3.602, QUANTITY='HRR'/

&DEVC ID='hrrpuv_x65', XB=1.134,1.215,-4.05,4.05,-1.42,3.602, QUANTITY='HRR'/

&DEVC ID='hrrpuv_x66', XB=1.215,1.296,-4.05,4.05,-1.42,3.602, QUANTITY='HRR'/

&DEVC ID='hrrpuv_x67', XB=1.296,1.377,-4.05,4.05,-1.42,3.602, QUANTITY='HRR'/

&DEVC ID='hrrpuv_x68', XB=1.377,1.458,-4.05,4.05,-1.42,3.602, QUANTITY='HRR'/

&DEVC ID='hrrpuv_x69', XB=1.458,1.539,-4.05,4.05,-1.42,3.602, QUANTITY='HRR'/

&DEVC ID='hrrpuv_x70', XB=1.539,1.62,-4.05,4.05,-1.42,3.602, QUANTITY='HRR'/

&DEVC ID='hrrpuv_x71', XB=1.62,1.701,-4.05,4.05,-1.42,3.602, QUANTITY='HRR'/

&DEVC ID='hrrpuv_x72', XB=1.701,1.782,-4.05,4.05,-1.42,3.602, QUANTITY='HRR'/

&DEVC ID='hrrpuv_x73', XB=1.782,1.863,-4.05,4.05,-1.42,3.602, QUANTITY='HRR'/

&DEVC ID='hrrpuv_x74', XB=1.863,1.944,-4.05,4.05,-1.42,3.602, QUANTITY='HRR'/

&DEVC ID='hrrpuv_x75', XB=1.944,2.025,-4.05,4.05,-1.42,3.602, QUANTITY='HRR'/

&DEVC ID='hrrpuv_x76', XB=2.025,2.106,-4.05,4.05,-1.42,3.602, QUANTITY='HRR'/

&DEVC ID='hrrpuv_x77', XB=2.106,2.187,-4.05,4.05,-1.42,3.602, QUANTITY='HRR'/

&DEVC ID='hrrpuv_x78', XB=2.187,2.268,-4.05,4.05,-1.42,3.602, QUANTITY='HRR'/

&DEVC ID='hrrpuv_x79', XB=2.268,2.349,-4.05,4.05,-1.42,3.602, QUANTITY='HRR'/

&DEVC ID='hrrpuv_x80', XB=2.349,2.43,-4.05,4.05,-1.42,3.602, QUANTITY='HRR'/

&DEVC ID='hrrpuv_x81', XB=2.43,2.511,-4.05,4.05,-1.42,3.602, QUANTITY='HRR'/

&DEVC ID='hrrpuv_x82', XB=2.511,2.592,-4.05,4.05,-1.42,3.602, QUANTITY='HRR'/

&DEVC ID='hrrpuv_x83', XB=2.592,2.673,-4.05,4.05,-1.42,3.602, QUANTITY='HRR'/

&DEVC ID='hrrpuv_x84', XB=2.673,2.754,-4.05,4.05,-1.42,3.602, QUANTITY='HRR'/

&DEVC ID='hrrpuv_x85', XB=2.754,2.835,-4.05,4.05,-1.42,3.602, QUANTITY='HRR'/

&DEVC ID='hrrpuv_x86', XB=2.835,2.916,-4.05,4.05,-1.42,3.602, QUANTITY='HRR'/

&DEVC ID='hrrpuv_x87', XB=2.916,2.997,-4.05,4.05,-1.42,3.602, QUANTITY='HRR'/

&DEVC ID='hrrpuv_x88', XB=2.997,3.078,-4.05,4.05,-1.42,3.602, QUANTITY='HRR'/

&DEVC ID='hrrpuv_x89', XB=3.078,3.159,-4.05,4.05,-1.42,3.602, QUANTITY='HRR'/

&DEVC ID='hrrpuv_x90', XB=3.159,3.24,-4.05,4.05,-1.42,3.602, QUANTITY='HRR'/

&DEVC ID='hrrpuv_x91', XB=3.24,3.321,-4.05,4.05,-1.42,3.602, QUANTITY='HRR'/

&DEVC ID='hrrpuv_x92', XB=3.321,3.402,-4.05,4.05,-1.42,3.602, QUANTITY='HRR'/

&DEVC ID='hrrpuv_x93', XB=3.402,3.483,-4.05,4.05,-1.42,3.602, QUANTITY='HRR'/

&DEVC ID='hrrpuv_x94', XB=3.483,3.564,-4.05,4.05,-1.42,3.602, QUANTITY='HRR'/

&DEVC ID='hrrpuv_x95', XB=3.564,3.645,-4.05,4.05,-1.42,3.602, QUANTITY='HRR'/

&DEVC ID='hrrpuv_x96', XB=3.645,3.726,-4.05,4.05,-1.42,3.602, QUANTITY='HRR'/

&DEVC ID='hrrpuv_x97', XB=3.726,3.807,-4.05,4.05,-1.42,3.602, QUANTITY='HRR'/

&DEVC ID='hrrpuv_x98', XB=3.807,3.888,-4.05,4.05,-1.42,3.602, QUANTITY='HRR'/

&DEVC ID='hrrpuv_x99', XB=3.888,3.969,-4.05,4.05,-1.42,3.602, QUANTITY='HRR'/

&DEVC ID='hrrpuv_x100', XB=3.969,4.05,-4.05,4.05,-1.42,3.602, QUANTITY='HRR'/

&DEVC ID='hrrpuv_y1', XB=-4.05,4.05,-4.05,-3.969,-1.42,3.602, QUANTITY='HRR'/

&DEVC ID='hrrpuv_y2', XB=-4.05,4.05,-3.969,-3.888,-1.42,3.602, QUANTITY='HRR'/

&DEVC ID='hrrpuv_y3', XB=-4.05,4.05,-3.888,-3.807,-1.42,3.602, QUANTITY='HRR'/

&DEVC ID='hrrpuv_y4', XB=-4.05,4.05,-3.807,-3.726,-1.42,3.602, QUANTITY='HRR'/

&DEVC ID='hrrpuv_y5', XB=-4.05,4.05,-3.726,-3.645,-1.42,3.602, QUANTITY='HRR'/

&DEVC ID='hrrpuv_y6', XB=-4.05,4.05,-3.645,-3.564,-1.42,3.602, QUANTITY='HRR'/

&DEVC ID='hrrpuv_y7', XB=-4.05,4.05,-3.564,-3.483,-1.42,3.602, QUANTITY='HRR'/

&DEVC ID='hrrpuv_y8', XB=-4.05,4.05,-3.483,-3.402,-1.42,3.602, QUANTITY='HRR'/

&DEVC ID='hrrpuv_y9', XB=-4.05,4.05,-3.402,-3.321,-1.42,3.602, QUANTITY='HRR'/

&DEVC ID='hrrpuv_y10', XB=-4.05,4.05,-3.321,-3.24,-1.42,3.602, QUANTITY='HRR'/

&DEVC ID='hrrpuv_y11', XB=-4.05,4.05,-3.24,-3.159,-1.42,3.602, QUANTITY='HRR'/

&DEVC ID='hrrpuv_y12', XB=-4.05,4.05,-3.159,-3.078,-1.42,3.602, QUANTITY='HRR'/

&DEVC ID='hrrpuv_y13', XB=-4.05,4.05,-3.078,-2.997,-1.42,3.602, QUANTITY='HRR'/

&DEVC ID='hrrpuv_y14', XB=-4.05,4.05,-2.997,-2.916,-1.42,3.602, QUANTITY='HRR'/

&DEVC ID='hrrpuv_y15', XB=-4.05,4.05,-2.916,-2.835,-1.42,3.602, QUANTITY='HRR'/

&DEVC ID='hrrpuv_y16', XB=-4.05,4.05,-2.835,-2.754,-1.42,3.602, QUANTITY='HRR'/

&DEVC ID='hrrpuv_y17', XB=-4.05,4.05,-2.754,-2.673,-1.42,3.602, QUANTITY='HRR'/

&DEVC ID='hrrpuv_y18', XB=-4.05,4.05,-2.673,-2.592,-1.42,3.602, QUANTITY='HRR'/

&DEVC ID='hrrpuv_y19', XB=-4.05,4.05,-2.592,-2.511,-1.42,3.602, QUANTITY='HRR'/

&DEVC ID='hrrpuv_y20', XB=-4.05,4.05,-2.511,-2.43,-1.42,3.602, QUANTITY='HRR'/

&DEVC ID='hrrpuv_y21', XB=-4.05,4.05,-2.43,-2.349,-1.42,3.602, QUANTITY='HRR'/

&DEVC ID='hrrpuv_y22', XB=-4.05,4.05,-2.349,-2.268,-1.42,3.602, QUANTITY='HRR'/

&DEVC ID='hrrpuv_y23', XB=-4.05,4.05,-2.268,-2.187,-1.42,3.602, QUANTITY='HRR'/

&DEVC ID='hrrpuv_y24', XB=-4.05,4.05,-2.187,-2.106,-1.42,3.602, QUANTITY='HRR'/

&DEVC ID='hrrpuv_y25', XB=-4.05,4.05,-2.106,-2.025,-1.42,3.602, QUANTITY='HRR'/

&DEVC ID='hrrpuv_y26', XB=-4.05,4.05,-2.025,-1.944,-1.42,3.602, QUANTITY='HRR'/

&DEVC ID='hrrpuv_y27', XB=-4.05,4.05,-1.944,-1.863,-1.42,3.602, QUANTITY='HRR'/

&DEVC ID='hrrpuv_y28', XB=-4.05,4.05,-1.863,-1.782,-1.42,3.602, QUANTITY='HRR'/

&DEVC ID='hrrpuv_y29', XB=-4.05,4.05,-1.782,-1.701,-1.42,3.602, QUANTITY='HRR'/

&DEVC ID='hrrpuv_y30', XB=-4.05,4.05,-1.701,-1.62,-1.42,3.602, QUANTITY='HRR'/

&DEVC ID='hrrpuv_y31', XB=-4.05,4.05,-1.62,-1.539,-1.42,3.602, QUANTITY='HRR'/

&DEVC ID='hrrpuv_y32', XB=-4.05,4.05,-1.539,-1.458,-1.42,3.602, QUANTITY='HRR'/

&DEVC ID='hrrpuv_y33', XB=-4.05,4.05,-1.458,-1.377,-1.42,3.602, QUANTITY='HRR'/

&DEVC ID='hrrpuv_y34', XB=-4.05,4.05,-1.377,-1.296,-1.42,3.602, QUANTITY='HRR'/

&DEVC ID='hrrpuv_y35', XB=-4.05,4.05,-1.296,-1.215,-1.42,3.602, QUANTITY='HRR'/

&DEVC ID='hrrpuv_y36', XB=-4.05,4.05,-1.215,-1.134,-1.42,3.602, QUANTITY='HRR'/

&DEVC ID='hrrpuv_y37', XB=-4.05,4.05,-1.134,-1.053,-1.42,3.602, QUANTITY='HRR'/

&DEVC ID='hrrpuv_y38', XB=-4.05,4.05,-1.053,-0.972,-1.42,3.602, QUANTITY='HRR'/

&DEVC ID='hrrpuv_y39', XB=-4.05,4.05,-0.972,-0.891,-1.42,3.602, QUANTITY='HRR'/

&DEVC ID='hrrpuv_y40', XB=-4.05,4.05,-0.891,-0.81,-1.42,3.602, QUANTITY='HRR'/

&DEVC ID='hrrpuv_y41', XB=-4.05,4.05,-0.81,-0.729,-1.42,3.602, QUANTITY='HRR'/

&DEVC ID='hrrpuv_y42', XB=-4.05,4.05,-0.729,-0.648,-1.42,3.602, QUANTITY='HRR'/

&DEVC ID='hrrpuv_y43', XB=-4.05,4.05,-0.648,-0.567,-1.42,3.602, QUANTITY='HRR'/

&DEVC ID='hrrpuv_y44', XB=-4.05,4.05,-0.567,-0.486,-1.42,3.602, QUANTITY='HRR'/

&DEVC ID='hrrpuv_y45', XB=-4.05,4.05,-0.486,-0.405,-1.42,3.602, QUANTITY='HRR'/

&DEVC ID='hrrpuv_y46', XB=-4.05,4.05,-0.405,-0.324,-1.42,3.602, QUANTITY='HRR'/

&DEVC ID='hrrpuv_y47', XB=-4.05,4.05,-0.324,-0.243,-1.42,3.602, QUANTITY='HRR'/

&DEVC ID='hrrpuv_y48', XB=-4.05,4.05,-0.243,-0.162,-1.42,3.602, QUANTITY='HRR'/

&DEVC ID='hrrpuv_y49', XB=-4.05,4.05,-0.162,-0.081,-1.42,3.602, QUANTITY='HRR'/

&DEVC ID='hrrpuv_y50', XB=-4.05,4.05,-0.081,0.0,-1.42,3.602, QUANTITY='HRR'/

&DEVC ID='hrrpuv_y51', XB=-4.05,4.05,0.0,0.081,-1.42,3.602, QUANTITY='HRR'/

&DEVC ID='hrrpuv_y52', XB=-4.05,4.05,0.081,0.162,-1.42,3.602, QUANTITY='HRR'/

&DEVC ID='hrrpuv_y53', XB=-4.05,4.05,0.162,0.243,-1.42,3.602, QUANTITY='HRR'/

&DEVC ID='hrrpuv_y54', XB=-4.05,4.05,0.243,0.324,-1.42,3.602, QUANTITY='HRR'/

&DEVC ID='hrrpuv_y55', XB=-4.05,4.05,0.324,0.405,-1.42,3.602, QUANTITY='HRR'/

&DEVC ID='hrrpuv_y56', XB=-4.05,4.05,0.405,0.486,-1.42,3.602, QUANTITY='HRR'/

&DEVC ID='hrrpuv_y57', XB=-4.05,4.05,0.486,0.567,-1.42,3.602, QUANTITY='HRR'/

&DEVC ID='hrrpuv_y58', XB=-4.05,4.05,0.567,0.648,-1.42,3.602, QUANTITY='HRR'/

&DEVC ID='hrrpuv_y59', XB=-4.05,4.05,0.648,0.729,-1.42,3.602, QUANTITY='HRR'/

&DEVC ID='hrrpuv_y60', XB=-4.05,4.05,0.729,0.81,-1.42,3.602, QUANTITY='HRR'/

&DEVC ID='hrrpuv_y61', XB=-4.05,4.05,0.81,0.891,-1.42,3.602, QUANTITY='HRR'/

&DEVC ID='hrrpuv_y62', XB=-4.05,4.05,0.891,0.972,-1.42,3.602, QUANTITY='HRR'/

&DEVC ID='hrrpuv_y63', XB=-4.05,4.05,0.972,1.053,-1.42,3.602, QUANTITY='HRR'/

&DEVC ID='hrrpuv_y64', XB=-4.05,4.05,1.053,1.134,-1.42,3.602, QUANTITY='HRR'/

&DEVC ID='hrrpuv_y65', XB=-4.05,4.05,1.134,1.215,-1.42,3.602, QUANTITY='HRR'/

&DEVC ID='hrrpuv_y66', XB=-4.05,4.05,1.215,1.296,-1.42,3.602, QUANTITY='HRR'/

&DEVC ID='hrrpuv_y67', XB=-4.05,4.05,1.296,1.377,-1.42,3.602, QUANTITY='HRR'/

&DEVC ID='hrrpuv_y68', XB=-4.05,4.05,1.377,1.458,-1.42,3.602, QUANTITY='HRR'/

&DEVC ID='hrrpuv_y69', XB=-4.05,4.05,1.458,1.539,-1.42,3.602, QUANTITY='HRR'/

&DEVC ID='hrrpuv_y70', XB=-4.05,4.05,1.539,1.62,-1.42,3.602, QUANTITY='HRR'/

&DEVC ID='hrrpuv_y71', XB=-4.05,4.05,1.62,1.701,-1.42,3.602, QUANTITY='HRR'/

&DEVC ID='hrrpuv_y72', XB=-4.05,4.05,1.701,1.782,-1.42,3.602, QUANTITY='HRR'/

&DEVC ID='hrrpuv_y73', XB=-4.05,4.05,1.782,1.863,-1.42,3.602, QUANTITY='HRR'/

&DEVC ID='hrrpuv_y74', XB=-4.05,4.05,1.863,1.944,-1.42,3.602, QUANTITY='HRR'/

&DEVC ID='hrrpuv_y75', XB=-4.05,4.05,1.944,2.025,-1.42,3.602, QUANTITY='HRR'/

&DEVC ID='hrrpuv_y76', XB=-4.05,4.05,2.025,2.106,-1.42,3.602, QUANTITY='HRR'/

&DEVC ID='hrrpuv_y77', XB=-4.05,4.05,2.106,2.187,-1.42,3.602, QUANTITY='HRR'/

&DEVC ID='hrrpuv_y78', XB=-4.05,4.05,2.187,2.268,-1.42,3.602, QUANTITY='HRR'/

&DEVC ID='hrrpuv_y79', XB=-4.05,4.05,2.268,2.349,-1.42,3.602, QUANTITY='HRR'/

&DEVC ID='hrrpuv_y80', XB=-4.05,4.05,2.349,2.43,-1.42,3.602, QUANTITY='HRR'/

&DEVC ID='hrrpuv_y81', XB=-4.05,4.05,2.43,2.511,-1.42,3.602, QUANTITY='HRR'/

&DEVC ID='hrrpuv_y82', XB=-4.05,4.05,2.511,2.592,-1.42,3.602, QUANTITY='HRR'/

&DEVC ID='hrrpuv_y83', XB=-4.05,4.05,2.592,2.673,-1.42,3.602, QUANTITY='HRR'/

&DEVC ID='hrrpuv_y84', XB=-4.05,4.05,2.673,2.754,-1.42,3.602, QUANTITY='HRR'/

&DEVC ID='hrrpuv_y85', XB=-4.05,4.05,2.754,2.835,-1.42,3.602, QUANTITY='HRR'/

&DEVC ID='hrrpuv_y86', XB=-4.05,4.05,2.835,2.916,-1.42,3.602, QUANTITY='HRR'/

&DEVC ID='hrrpuv_y87', XB=-4.05,4.05,2.916,2.997,-1.42,3.602, QUANTITY='HRR'/

&DEVC ID='hrrpuv_y88', XB=-4.05,4.05,2.997,3.078,-1.42,3.602, QUANTITY='HRR'/

&DEVC ID='hrrpuv_y89', XB=-4.05,4.05,3.078,3.159,-1.42,3.602, QUANTITY='HRR'/

&DEVC ID='hrrpuv_y90', XB=-4.05,4.05,3.159,3.24,-1.42,3.602, QUANTITY='HRR'/

&DEVC ID='hrrpuv_y91', XB=-4.05,4.05,3.24,3.321,-1.42,3.602, QUANTITY='HRR'/

&DEVC ID='hrrpuv_y92', XB=-4.05,4.05,3.321,3.402,-1.42,3.602, QUANTITY='HRR'/

&DEVC ID='hrrpuv_y93', XB=-4.05,4.05,3.402,3.483,-1.42,3.602, QUANTITY='HRR'/

&DEVC ID='hrrpuv_y94', XB=-4.05,4.05,3.483,3.564,-1.42,3.602, QUANTITY='HRR'/

&DEVC ID='hrrpuv_y95', XB=-4.05,4.05,3.564,3.645,-1.42,3.602, QUANTITY='HRR'/

&DEVC ID='hrrpuv_y96', XB=-4.05,4.05,3.645,3.726,-1.42,3.602, QUANTITY='HRR'/

&DEVC ID='hrrpuv_y97', XB=-4.05,4.05,3.726,3.807,-1.42,3.602, QUANTITY='HRR'/

&DEVC ID='hrrpuv_y98', XB=-4.05,4.05,3.807,3.888,-1.42,3.602, QUANTITY='HRR'/

&DEVC ID='hrrpuv_y99', XB=-4.05,4.05,3.888,3.969,-1.42,3.602, QUANTITY='HRR'/

&DEVC ID='hrrpuv_y100', XB=-4.05,4.05,3.969,4.05,-1.42,3.602, QUANTITY='HRR'/

/********************* MATERIAL & SURFACE *********************************

&MATL ID   = 'ASBESTOS-CEMENT'

    DENSITY   = 1400.

    CONDUCTIVITY   = 0.744

    SPECIFIC_HEAT   = 0.84 /

&MATL ID   = 'PLYWOOD'

    DENSITY   = 690.

    CONDUCTIVITY   = 0.13

    SPECIFIC_HEAT   = 1.215 /

&MATL ID   = 'MARINITE'

    DENSITY   = 737.

    CONDUCTIVITY   = 0.12

    SPECIFIC_HEAT   = 1.424 /

&MATL ID   = 'STEEL'

    EMISSIVITY   = 0.5

    DENSITY   = 7850.

L

```
          CONDUCTIVITY      = 45.8

          SPECIFIC_HEAT     = 0.46 /

&SURF ID            = 'FLOOR1'

     RGB            = 170,170,170

       MATL_ID        = 'ASBESTOS-CEMENT'

       THICKNESS       = 0.0095 /

&SURF ID            = 'FLOOR2'

       COLOR         = 'BRICK'

       MATL_ID        = 'PLYWOOD'

       THICKNESS       = 0.025 /

&SURF ID            = 'BURNER'

       COLOR         = 'BLACK'

       MATL_ID        = 'STEEL'

       GEOMETRY          = 'CYLINDRICAL'

       THICKNESS       = 0.005 /

&SURF ID            = 'ROOF1'

       COLOR         = 'GRAY'

       BACKING          = 'EXPOSED'

       MATL_ID        = 'MARINITE'

       THICKNESS       = 0.0127 /

&SURF ID            = 'ROOF2'

       COLOR         = 'BLACK'

       MATL_ID        = 'STEEL'

       THICKNESS       = 0.025 /

&TAIL /

/********************* End *****************************************
```

M

8.3 Appendix C

MATLAB script used for placing devices in FDS

```matlab
clear all

%%%%%%% INPUT %%%%%%%%%%%%%

%NB: fire must be place in center of domain (0,0,0)

horizontal = 1; %logical expression; if value == 0 then vertical direction
is printed

dx = 0.1; %grid dimension in meters, dx=dxy=dz
x_min = -6.5; %[m]
x_max = 6.5; %[m]
z_min = -1.42; %[m]
z_max = 5.48; %[m]


%%%%%%% PROGRAM %%%%%%%%%%%%%

y_min = x_min; %[m]
y_max = x_max; %[m]

dy = dx;
dz = dx;

n_x = (x_max-x_min)/dx;
n_y = n_x;
n_z = (z_max-z_min)/dz;

if horizontal == 1
    x(1) = x_min;
    for i=1:n_x+1
        x(i+1) = x(i) + dx;
        disp(['&DEVC ID=''hrrpuv_x' num2str(i) ''', XB=' num2str(x(i)) ','
num2str(x(i+1)) ',' num2str(y_min) ',' num2str(y_max) ',' num2str(z_min)
',' num2str(z_max) ', QUANTITY=''HRR''/']) %center point
    end
    y(1) = y_min;
    for i=1:n_y+1
        y(i+1) = y(i) + dy;
        disp(['&DEVC ID=''hrrpuv_y' num2str(i) ''', XB=' num2str(x_min) ','
num2str(x_max) ',' num2str(y(i)) ',' num2str(y(i+1)) ',' num2str(z_min) ','
num2str(z_max) ', QUANTITY=''HRR''/']) %center point
    end
else %vetical == .true.
    z(1) = z_min;
    for i=1:n_z+1
        z(i+1) = z(i) + dz;
        disp(['&DEVC ID=''hrrpuv_z' num2str(i) ''', XB=' num2str(x_min) ','
num2str(x_max) ',' num2str(y_min) ',' num2str(y_max) ',' num2str(z(i)) ','
num2str(z(i+1)) ', QUANTITY=''HRR''/']) %center point
    end
end
```

8.4 Appendix D

MATLAB script used for calculating mean flame extension length

```matlab
clear all

file='full-4500-100s-newroof.xlsx';

[num,txt,raw] = xlsread(file);

horizontal = 1; %if == 0 then vertical flame height i calculated

tstep = 5001; %number of timesteps
xmpnt = 80; %measuring points
zmpnt = 0; %measuring points
dx = 0.081; %størrelse griddcelle meter

x_max=6.48; %bredde + og - for center i 0
y_max=x_max;

dy = dx;
dz = dx;%må gjøres om for vertikal
ympnt = xmpnt; %measuring points
x = x_max -(dx*0.5); %possition av siste device
y = y_max -(dy*0.5); %
z = 180 - (dz*0.5); %ymax
criteria=0.99;
%sum1=0.0;
%sumold = sum1;


%x negativ retting

for i = 1:tstep
    t(i) = num(i,1);%viser til at tidsstegen finnes i kollonne 1 i
excelarket

    for j = 1:xmpnt;
        hrrx1(i,j) = num(i,j+1);%viser at hrr for hvert tidssteg finnes fra
kolonne 2 og bort over
    end
end
hrr_totx1=sum(hrrx1,2);
i=2;%Må settes til 1 så in if setting med når hrr_tot=0 = poss=0
while i<=tstep;
    j=xmpnt;
    hrr=hrrx1(i,j);
    while j<=xmpnt;
        if hrr<=hrr_totx1(i)*criteria;
        hrr_old=hrr;
        hrr=hrr+hrrx1(i,j-1);
        else
        possx1(i) = ((xmpnt-j)-1)*dx + ((xmpnt-j)*dx - ((xmpnt-j)-
1)*dx)*(criteria*hrr_totx1(i) - hrr_old)/(hrr-hrr_old);
        j=xmpnt+2;
        end
        j = j - 1;
    end
    i=i+1;
end
```

O

```matlab
distx1=mean(possx1([2503:tstep]));
hrr_tot_mean_x1=mean(hrr_totx1);
%x possitiv retting

for i = 1:tstep
    t(i) = num(i,1);%viser til at tidsstegen finnes i kollonne 1 i
excelarket

    for j = 1:xmpnt;
        hrrx2(i,j) = num(i,j+xmpnt);%viser at hrr for hvert tidssteg finnes
fra kolonne 2 og bort over
    end
end
hrr_totx2=sum(hrrx2,2);
i=2;
while i<=tstep;
    j=1;
    hrr=hrrx2(i,j);
    while j<xmpnt;
        if hrr<=hrr_totx2(i)*criteria;
        hrr_old=hrr;
        hrr=hrr+hrrx2(i,j+1);
        else
        possx2(i) = (j-1)*dx + (j*dx - (j-1)*dx)*(criteria*hrr_totx2(i) -
hrr_old)/(hrr-hrr_old);
        j=xmpnt+1;
        end
        j = j + 1;
    end
    i=i+1;
end
hrr_tot_mean_x2=mean(hrr_totx2);
distx2=mean(possx2([2503:tstep]));

 %y negativ retting

for i = 1:tstep
    t(i) = num(i,1);%viser til at tidsstegen finnes i kollonne 1 i
excelarket

    for j = 1:ympnt;
        hrry1(i,j) = num(i,j+(2*xmpnt));%viser at hrr for hvert tidssteg
finnes fra kolonne 2 og bort over
    end
end
hrr_toty1=sum(hrry1,2);
i=2;%Må settes til 1 så in if setting med når hrr_tot=0 = poss=0
while i<=tstep;
    j=ympnt;
    hrr=hrry1(i,j);
    while j<=ympnt;
        if hrr<=hrr_toty1(i)*criteria;
        hrr_old=hrr;
        hrr=hrr+hrry1(i,j-1);
        else
        possy1(i) = ((ympnt-j)-1)*dx + ((ympnt-j)*dx - ((ympnt-j)-
1)*dx)*(criteria*hrr_toty1(i) - hrr_old)/(hrr-hrr_old);
        j=ympnt+2;
        end
```

```matlab
        j = j - 1;
    end
    i=i+1;
end
hrr_tot_mean_y1=mean(hrr_toty1);
disty1=mean(possy1([2503:tstep]));

%y possitiv retting

for i = 1:tstep
    t(i) = num(i,1);%viser til at tidsstegen finnes i kollonne 1 i
excelarket

    for j = 1:ympnt;
        hrry2(i,j) = num(i,j+(ympnt+(2*xmpnt)));%viser at hrr for hvert
tidssteg finnes fra kolonne 2 og bort over
    end
end
hrr_toty2=sum(hrry2,2);
i=2;
while i<=tstep;
    j=1;
    hrr=hrry2(i,j);
    while j<ympnt;
        if hrr<=hrr_toty2(i)*criteria;
        hrr_old=hrr;
        hrr=hrr+hrry2(i,j+1);
        else
        possy2(i) = (j-1)*dx + (j*dx - (j-1)*dx)*(criteria*hrr_toty2(i) -
hrr_old)/(hrr-hrr_old);
        j=ympnt+1;
        end
        j = j + 1;
    end
    i=i+1;
end
hrr_tot_mean_y2=mean(hrr_toty2);
disty2=mean(possy2([2503:tstep]));

flame_radius=((distx1+distx2+disty1+disty2)/4)
```

Q

8.5 Appendix E

MATLAB script used to calculating mean flame height

```matlab
clear all

file='open-23.2-0.01-100s.xlsx';

[num,txt,raw] = xlsread(file);

horizontal = 1; %if == 0 then vertical flame height i calculated

tstep = 5001; %number of timesteps
zmpnt = 200; %measuring points
dz = 0.01; %størrelse griddcelle meter

x_max=1; %bredde + og - for center i 0
y_max=x_max;
z_max=2.0;




z = z_max - (dz*0.5); %ymax
criteria=0.99;
%sum1=0.0;
%sumold = sum1;

%x possitiv retting

for i = 1:tstep
    t(i) = num(i,1);%viser til at tidsstegen finnes i kollonne 1 i
excelarket

    for j = 1:zmpnt;
        hrrz(i,j) = num(i,j);%viser at hrr for hvert tidssteg finnes fra
kolonne 2 og bort over
    end
end
hrr_totz=sum(hrrz,2);
i=2;
while i<=tstep;
    j=1;
    hrr=hrrz(i,j);
    while j<zmpnt;
        if hrr<=hrr_totz(i)*criteria;
        hrr_old=hrr;
        hrr=hrr+hrrz(i,j+1);
        else
        possz(i) = (j-1)*dz + (j*dz - (j-1)*dz)*(criteria*hrr_totz(i) -
hrr_old)/(hrr-hrr_old);
        j=zmpnt+1;
        end
        j = j + 1;
    end
    i=i+1;
end

distz=mean(possz([2503:5001]));
flame_height=(distz-0.3843)
```

Results from performed simulations in FDS

Simulation 23.2 kW 100s 0.0405m

Simulation				Heskestad				Deviation					
				Flameradius [m]				Flameradius		Flameheight		Effect	Burner size
Mean flameradius [m]	Mean flameheight [m]	Roofheight [m]	Expected radius using formula [m]	0.88	0.95	1.05	Flameheight [m]	[m]	[%]	[m]	[%]	[kW]	[m]
0.12	0.46	0.56	-0.09	0.10	0.11	0.12	0.67	0.02	-12.73	-0.21	45.13	23.20	0.15

Simulation 46.2 kW 100s 0.0405m

Simulation				Heskestad				Deviation					
				Flameradius [m]				Flameradius		Flameheight		Effect	Burner size
Mean flameradius [m]	Mean flameheight [m]	Roofheight [m]	Expected radius using formula	0.88	0.95	1.05	Flameheight [m]	[m]	[%]	[m]	[%]	[kW]	[m]
0.23	2.74	0.56	2.07	0.33	0.36	0.39	0.94	-0.13	54.86	1.80	-65.79	46.20	0.15

Simulation 92.6 kW 100s 0.0405m

Simulation				Heskestad				Deviation					
				Flameradius [m]				Flameradius		Flameheight		Effect	Burner size
Mean flameradius [m]	Mean flameheight [m]	Roofheight [m]	Expected radius using formula	0.88	0.95	1.05	Flameheight [m]	[m]	[%]	[m]	[%]	[kW]	[m]
0.20	1.00	0.92	0.08	0.19	0.20	0.22	1.13	0.00	2.21	-0.13	12.81	92.60	0.30

Simulation 185 kW 100s 0.0405m

Simulation				Heskestad				Deviation					
				Flameradius [m]				Flameradius		Flameheight		Effect	Burner size
Mean flameradius [m]	Mean flameheight [m]	Roofheight [m]	Expected radius using formula	0.88	0.95	1.05	Flameheight [m]	[m]	[%]	[m]	[%]	[kW]	[m]
0.50	1.42	0.92	0.48	0.59	0.64	0.70	1.59	-0.14	28.38	-0.17	11.62	185.00	0.30

Simulation 382 kW 100s 0.0405m

Simulation				Heskestad				Deviation					
				Flameradius [m]				Flameradius		Flameheight		Effect	Burner size
Mean flameradius [m]	Mean flameheight [m]	Roofheight [m]	Expected radius using formula	0.88	0.95	1.05	Flameheight [m]	[m]	[%]	[m]	[%]	[kW]	[m]
0.57	2.01	1.51	0.48	0.35	0.38	0.42	1.91	0.18	-32.43	0.10	-5.03	382.00	0.61

Simulation 764 kW 100s 0.0405m

Simulation				Heskestad				Deviation					
				Flameradius [m]				Flameradius		Flameheight		Effect	Burner size
Mean flameradius [m]	Mean flameheight [m]	Roofheight [m]	Expected radius using formula	0.88	0.95	1.05	Flameheight [m]	[m]	[%]	[m]	[%]	[kW]	[m]
1.15	2.74	1.51	1.17	1.07	1.15	1.27	2.72	0.00	0.25	0.02	-0.64	764.00	0.61

T

Simulation 764 kW 100s 0.081m

Simulation				Heskestad				Deviation					
				Flameradius [m]				Flameradius		Flameheight		Effect	Burner size
Mean flameradius [m]	Mean flameheight [m]	Roofheight [m]	Expected radius using formula	0.88	0.95	1.05	Flameheight [m]	[m]	[%]	[m]	[%]	[kW]	[m]
0.82	2.74	1.51	1.17	1.07	1.15	1.27	2.72	-0.33	40.82	0.02	-0.64	764.00	0.61

Simulation 764 kW 100s 0.0405m 0.92m roof

Simulation				Heskestad				Deviation					
				Flameradius [m]				Flameradius		Flameheight		Effect	Burner size
Mean flameradius [m]	Mean flameheight [m]	Roofheight [m]	Expected radius using formula	0.88	0.95	1.05	Flameheight [m]	[m]	[%]	[m]	[%]	[kW]	[m]
1.63	2.74	0.92	1.73	1.59	1.71	1.89	2.72	-0.08	4.79	0.02	-0.64	764.00	0.61

Simulation 972 kW 100s 0.0405m

Simulation				Heskestad				Deviation					
				Flameradius [m]				Flameradius		Flameheight		Effect	Burner size
Mean flameradius [m]	Mean flameheight [m]	Roofheight [m]	Expected radius using formula	0.88	0.95	1.05	Flameheight [m]	[m]	[%]	[m]	[%]	[kW]	[m]
1.41	2.99	1.51	1.41	1.36	1.47	1.63	3.06	-0.07	4.80	-0.07	2.25	972.00	0.61

U

Simulation 1500 kW 100s 0.0405m

Simulation				Heskestad				Deviation					
				Flameradius [m]				Flameradius		Flameheight		Effect	Burner size
Mean flameradius [m]	Mean flameheight [m]	Roofheight [m]	Expected radius using formula	0.88	0.95	1.05	Flameheight [m]	[m]	[%]	[m]	[%]	[kW]	[m]
1.94	3.57	1.51	1.96	1.76	1.90	2.10	3.51	0.04	-2.08	0.06	-1.56	1500.00	0.85

Simulation 2000 kW 100s 0.0405m

Simulation				Heskestad				Deviation					
				Flameradius [m]				Flameradius		Flameheight		Effect	Burner size
Mean flameradius [m]	Mean flameheight [m]	Roofheight [m]	Expected radius using formula	0.88	0.95	1.05	Flameheight [m]	[m]	[%]	[m]	[%]	[kW]	[m]
1.91	4.14	2.00	2.03	1.67	1.80	1.99	3.89	0.12	-6.01	0.24	-5.87	2000.00	1.00

Simulation 2500 kW 100s 0.0675m

Simulation				Heskestad				Deviation					
				Flameradius [m]				Flameradius		Flameheight		Effect	Burner size
Mean flameradius [m]	Mean flameheight [m]	Roofheight [m]	Expected radius using formula	0.88	0.95	1.05	Flameheight [m]	[m]	[%]	[m]	[%]	[kW]	[m]
1.69	4.02	2.50	1.44	1.54	1.66	1.84	4.25	0.02	-1.31	-0.23	5.74	2500.00	1.10

Simulation 3000 kW 100s 0.075m

Simulation				Heskestad				Deviation					
				Flameradius [m]				Flameradius		Flameheight		Effect	Burner size
Mean flameradius [m]	Mean flameheight [m]	Roofheight [m]	Expected radius using formula	0.88	0.95	1.05	Flameheight [m]	[m]	[%]	[m]	[%]	[kW]	[m]
1.82	4.80	2.50	2.18	1.72	1.86	2.05	4.45	-0.04	1.95	0.34	-7.11	3000.00	1.30

Simulation 3500 kW 100s 0.081m

Simulation				Heskestad				Deviation					
				Flameradius [m]				Flameradius		Flameheight		Effect	Burner size
Mean flameradius [m]	Mean flameheight [m]	Roofheight [m]	Expected radius using formula	0.88	0.95	1.05	Flameheight [m]	[m]	[%]	[m]	[%]	[kW]	[m]
1.67	4.91	3.00	1.81	1.60	1.73	1.91	4.82	-0.06	3.47	0.08	-1.71	3500.00	1.30

Simulation 4000 kW 100s 0.081m

Simulation				Heskestad				Deviation					
				Flameradius [m]				Flameradius		Flameheight		Effect	Burner size
Mean flameradius [m]	Mean flameheight [m]	Roofheight [m]	Expected radius using formula	0.88	0.95	1.05	Flameheight [m]	[m]	[%]	[m]	[%]	[kW]	[m]
1.86	5.17	3.00	2.06	1.81	1.95	2.16	5.06	-0.09	4.94	0.11	-2.12	4000.00	1.40

W

Simulation 4500 kW 100s 0.081m

Simulation				Heskestad				Deviation					
				Flameradius [m]				Flameradius		Flameheight		Effect	Burner size
Mean flameradius [m]	Mean flameheight [m]	Roofheight [m]	Expected radius using formula	0.88	0.95	1.05	Flameheight [m]	[m]	[%]	[m]	[%]	[kW]	[m]
0.93	5.36	3.50	1.77	1.56	1.68	1.86	5.27	-0.75	81.14	0.09	-1.74	4500.00	1.50

Simulation 5000 kW 100s 0.09m

Simulation				Heskestad				Deviation					
				Flameradius [m]				Flameradius		Flameheight		Effect	Burner size
Mean flameradius [m]	Mean flameheight [m]	Roofheight [m]	Expected radius using formula	0.88	0.95	1.05	Flameheight [m]	[m]	[%]	[m]	[%]	[kW]	[m]
1.72	5.80	3.50	2.19	1.72	1.86	2.06	5.46	-0.14	8.27	0.34	-5.91	5000.00	1.60

Simulation 5500 kW 100s 0.1m

Simulation				Heskestad				Deviation					
				Flameradius [m]				Flameradius		Flameheight		Effect	Burner size
Mean flameradius [m]	Mean flameheight [m]	Roofheight [m]	Expected radius using formula	0.88	0.95	1.05	Flameheight [m]	[m]	[%]	[m]	[%]	[kW]	[m]
0.95	5.90	3.50	2.28	1.88	2.03	2.24	5.63	-1.08	113.91	0.27	-4.55	5500.00	1.70

X

Simulation 6000 kW 100s 0.1m

Simulation				Heskestad				Deviation					
				Flameradius [m]				Flameradius		Flameheight		Effect	Burner size
Mean flameradius [m]	Mean flameheight [m]	Roofheight [m]	Expected radius using formula	0.88	0.95	1.05	Flameheight [m]	[m]	[%]	[m]	[%]	[kW]	[m]
1.01	6.05	3.50	2.42	2.11	2.27	2.51	5.89	-1.26	124.71	0.15	-2.55	6000.00	1.70

Simulation 6500 kW 100s 0.1m

Simulation				Heskestad				Deviation					
				Flameradius [m]				Flameradius		Flameheight		Effect	Burner size
Mean flameradius [m]	Mean flameheight [m]	Roofheight [m]	Expected radius using formula	0.88	0.95	1.05	Flameheight [m]	[m]	[%]	[m]	[%]	[kW]	[m]
0.87	6.08	4.00	1.97	1.79	1.94	2.14	6.04	-1.07	122.41	0.04	-0.61	6500.00	1.80

Simulation 7000 kW 100s 0.1m

Simulation				Heskestad				Deviation					
				Flameradius [m]				Flameradius		Flameheight		Effect	Burner size
Mean flameradius [m]	Mean flameheight [m]	Roofheight [m]	Expected radius using formula	0.88	0.95	1.05	Flameheight [m]	[m]	[%]	[m]	[%]	[kW]	[m]
0.96	6.20	4.00	2.09	1.96	2.11	2.34	6.22	-1.15	120.12	-0.03	0.47	7000.00	1.85

Y

Simulation 23.2 kW 100s New Grid 0.01m

Simulation				Heskestad				Deviation					
				Flameradius [m]				Flameradius		Flameheight		Effect	Burner size
Mean flameradius [m]	Mean flameheight [m]	Roofheight [m]	Expected radius using formula	0.88	0.95	1.05	Flameheight [m]	[m]	[%]	[m]	[%]	[kW]	[m]
0.12	0.55	0.56	-0.01	0.10	0.11	0.12	0.67	0.01	-9.89	-0.12	21.47	23.20	0.15

Simulation 46.2 kW 100s New Grid 0.015 m

Simulation				Heskestad				Deviation					
				Flameradius [m]				Flameradius		Flameheight		Effect	Burner size
Mean flameradius [m]	Mean flameheight [m]	Roofheight [m]	Expected radius using formula	0.88	0.95	1.05	Flameheight [m]	[m]	[%]	[m]	[%]	[kW]	[m]
0.33	0.79	0.56	0.22	0.33	0.36	0.39	0.94	-0.03	8.99	-0.14	18.21	46.20	0.15

Simulation 382 kW 100s New Grid 0.03 m

Simulation				Heskestad				Deviation					
				Flameradius [m]				Flameradius		Flameheight		Effect	Burner size
Mean flameradius [m]	Mean flameheight [m]	Roofheight [m]	Expected radius using formula	0.88	0.95	1.05	Flameheight [m]	[m]	[%]	[m]	[%]	[kW]	[m]
0.56	2.01	1.51	0.48	0.35	0.38	0.42	1.91	0.18	-32.34	0.10	-4.86	382.00	0.61

z

Simulation 4500 kW 100s 0.081m New Roof

Simulation				Heskestad				Deviation					
				Flameradius [m]				Flameradius		Flameheight		Effect	Burner size
Mean flameradius [m]	Mean flameheight [m]	Roofheight [m]	Expected radius using formula	0.88	0.95	1.05	Flameheight [m]	[m]	[%]	[m]	[%]	[kW]	[m]
3.12	5.36	2.10	3.10	2.79	3.01	3.33	5.27	0.11	-3.51	0.09	-1.72	4500.00	1.50

Simulation 5000 kW 100s 0.09m New Roof

Simulation				Heskestad				Deviation					
				Flameradius [m]				Flameradius		Flameheight		Effect	Burner size
Mean flameradius [m]	Mean flameheight [m]	Roofheight [m]	Expected radius using formula	0.88	0.95	1.05	Flameheight [m]	[m]	[%]	[m]	[%]	[kW]	[m]
3.01	5.80	2.10	3.52	2.96	3.19	3.53	5.46	-0.18	5.98	0.34	-5.89	5000.00	1.60

Simulation 5500 kW 100s 0.1m New Roof

Simulation				Heskestad				Deviation					
				Flameradius [m]				Flameradius		Flameheight		Effect	Burner size
Mean flameradius [m]	Mean flameheight [m]	Roofheight [m]	Expected radius using formula	0.88	0.95	1.05	Flameheight [m]	[m]	[%]	[m]	[%]	[kW]	[m]
3.28	5.90	2.10	3.61	3.11	3.36	3.71	5.63	-0.07	2.28	0.27	-4.55	5500.00	1.70

Æ

Simulation 6000 kW 100s 0.1m New roof

Simulation				Heskestad				Deviation					
				Flameradius [m]				Flameradius		Flameheight		Effect	Burner size
Mean flameradius [m]	Mean flameheight [m]	Roofheight [m]	Expected radius using formula	0.88	0.95	1.05	Flameheight [m]	[m]	[%]	[m]	[%]	[kW]	[m]
3.34	6.05	2.32	3.54	3.14	3.39	3.75	5.89	-0.06	1.68	0.16	-2.60	6000.00	1.70

Simulation 6500 kW 100s 0.1m New roof

Simulation				Heskestad				Deviation					
				Flameradius [m]				Flameradius		Flameheight		Effect	Burner size
Mean flameradius [m]	Mean flameheight [m]	Roofheight [m]	Expected radius using formula	0.88	0.95	1.05	Flameheight [m]	[m]	[%]	[m]	[%]	[kW]	[m]
3.47	6.08	2.30	3.59	3.29	3.55	3.93	6.04	-0.08	2.38	0.04	-0.68	6500.00	1.80

Simulation 7000 kW 100s 0.1m New Roof

Simulation				Heskestad				Deviation					
				Flameradius [m]				Flameradius		Flameheight		Effect	Burner size
Mean flameradius [m]	Mean flameheight [m]	Roofheight [m]	Expected radius using formula	0.88	0.95	1.05	Flameheight [m]	[m]	[%]	[m]	[%]	[kW]	[m]
3.70	6.20	2.40	3.61	3.37	3.63	4.02	6.22	0.07	-1.77	-0.03	0.47	7000.00	1.85

Ø

8.7 Appendix G

Model error calculation results

Table 5 Calculations of precentral model error for performed flame extension simulations, flame height simulations, calculations performed using equation (1.2) and (1.4), and the expected flame extension using equation (1.4) and the simulated flame height as input quantity.

	Flame extension		Flame height		Expected radius	Simulering radius	Error	Equation 1.4
HRR	%	m	%	m	m	m	%	%
23.2	-9.89	0.01	21.47	-0.03	-0.01	0.12	-104.37	-104.84
46.2	8.99	-0.03	18.21	-0.14	0.22	0.33	-32.82	-38.36
92.6	2.21	0.00	12.81	-0.13	0.08	0.20	-59.81	-60.68
185.0	28.38	-0.14	11.62	-0.17	0.48	0.50	-3.33	-24.70
382.0	-32.34	0.18	-4.86	0.10	0.48	0.56	-15.91	24.28
764.0	0.25	0.00	-0.64	0.02	1.17	1.15	1.71	1.45
764.0	4.79	-0.08			1.73	1.63	5.82	0.98
972.0	4.80	-0.07	2.25	-0.07	1.41	1.41	0.25	-4.35
1500.0	-2.08	0.04	-1.56	0.06	1.96	1.94	0.65	2.79
2000.0	-6.01	0.12	-5.87	0.24	2.03	1.91	6.04	12.82
2500.0	-1.31	0.02	5.74	-0.23	1.44	1.69	-14.30	-13.17
3000.0	1.95	-0.04	-7.11	0.34	2.18	1.82	19.75	17.46
3500.0	3.47	-0.06	-1.71	0.08	1.81	1.67	8.24	4.61
4000.0	4.94	-0.09	-2.12	0.11	2.06	1.86	10.53	5.33
4500.0	-3.51	0.11	-1.74	0.09	3.10	3.12	-0.70	2.92
5000.0	5.98	-0.18	-5.91	0.34	3.52	3.01	16.77	10.18
5500.0	2.28	-0.07	-4.55	0.27	3.61	3.28	10.05	7.60
6000.0	1.68	-0.06	-2.55	0.15	3.54	3.34	6.17	4.41
6500.0	2.38	-0.08	-0.61	0.04	3.59	3.47	3.51	1.11
7000.0	-1.77	0.07	0.47	-0.03	3.61	3.70	-2.52	-0.77
Average percentage model error	0.76	-0.02	1.75	0.06			-7.21	-7.55
Variance	116.69	0.01	66.10	0.03			802.81	855.99
Standard percentage model error	10.80	0.09	8.13	0.16			28.33	29.26

Å